arTs Università degli Studi di Trieste
Archivio della ricerca – postprint

The clays involved in the 1963 Vajont landslide: Genesis and geomechanical implications

Paolo Paronuzzi [a], Alberto Bolla [a,*], Daniela Pinto [b], Davide Lenaz [c], Massimo Soccal [a]

[a] Dipartimento Politecnico di Ingegneria e Architettura, Università degli Studi di Udine, via Cotonificio 114, 33100 Udine, Italy
[b] Dipartimento di Scienze della Terra e Geoambientali, Università degli Studi di Bari A. Moro, via Orabona 4, 70125 Bari, Italy
[c] Dipartimento di Matematica e Geoscienze, Università degli Studi di Trieste, via Weiss 8, 34127 Trieste, Italy

ARTICLE INFO

Keywords:
Vajont landslide
Clay
Illite/Smectite mixed layer
Shear strength
Volcanic ash
Jurassic tephra

ABSTRACT

The catastrophic Vajont landslide that occurred on 9 October 1963 caused about 2000 deaths when 270–300 Mm^3 of rock and debris slid from the northern slope of Mt. Toc into the newly created artificial reservoir, displacing some huge water waves that flooded the nearby villages. The 1963 slide was an en-block remobilisation of a prehistoric rockslide lying on the southern reservoir bank. Basal sliding took place within a complex lithostratigraphic sequence of cherty–marly limestones and clay interbeds belonging to the Fonzaso Formation of Upper Jurassic age. In this work, we investigate the geological origin and provenance of the Vajont clays according to the results of mineralogical and geochemical analyses performed on several clay samples which were collected from the landslide failure surface and the same limestone sequence in the surrounding area. The sampled clayey materials contained variable amounts of clay minerals (36–96%), calcite (4–64%) and quartz (0–6%). The dominant clay minerals were illite/smectite (I/S) mixed layers with a high illite content (85–50%), which was consistent with the high percentage of K_2O (1.17–5.77%). The Vajont clays included in the Fonzaso Fm. can be referred to as K-bentonites and can be interpreted as distinct deposits of volcanoclastic materials (tephra), representing the sedimentary inputs of volcanic ashes that interrupted the "normal" calcareous sedimentation during the late Oxfordian–upper Tithonian (158–145 Ma). The soft clay interbeds played a different mechanical role in the occurrence of the prehistoric rockslide and the 1963 en-block remobilisation. When referring to the ancient slope failures, distinct clay-rich layers that were concentrated within some specific lithostratigraphic intervals of the Jurassic cherty limestone sequence caused a localised decrease in the available shear strength, allowing for relative shear displacements along the dip-slope bedding planes. This caused additional shear/tensile fracturing of limestone beds and the formation of a stepped basal failure surface. During the 1963 remobilisation, the clay layers contributed to the average shear strength decrease of the debris material forming the basal shear zone of the slide, but the main triggering factor was the increase in pore pressures caused by the reservoir-induced groundwater inflow.

1. Introduction

The 270–300 Mm^3 Vajont landslide (Fig. 1) was and still remains one of the largest mass movements in the Alps (Müller, 1964;Paronuzzi et al., 2013a). This catastrophic landslide occurred in the Vajont valley, in the South-eastern Alps, in the Friuli Venezia Giulia Region, about 120 km north to Venice (Italy). The Vajont valley is a prevailing E–W trend fluvio-glacial valley crossed by the Vajont stream, a tributary of the Piave river, which was dammed to construct a hydroelectric power plant. The 261.60 m-height concrete double-curvature arch dam was constructed between 1957 and 1960 in the narrow Vajont gorge eroded in the oolitic limestone of the Calcare del Vajont Formation of Middle Jurassic age and was the tallest dam in the world at that time (today, the 7th).

On 9 October 1963, a huge rock mass detached from the northern slope of Mt. Toc on the southern valley flank and slid as a coherent block into the reservoir. As Fig. 1 shows, the dam survived the impact, but the failed mass generated a number of waves that caused massive flooding and the complete destruction of surrounding towns and villages, especially downstream of the dam, resulting in the deaths of about 2000 people. On 12 February 2008, when launching the International Year of Planet Earth, the United Nations Educational, Scientific and Cultural

* Corresponding author.
E-mail address: alberto.bolla@uniud.it (A. Bolla).

Accepted 15 September 2021

Organization (UNESCO) cited the 1963 Vajont landslide as the worst man-made environmental disaster of all time (https://en.lswn.it/events/international-year-of-planet-earth-global-launch-event-12-13-february-2008/).

A new research project on the 1963 Vajont landslide was begun in 2000 with the aim of investigating the geological features of this particularly complex rockslide as well as to ascertain the causes and the possible trigger of the catastrophic slope failure. This research, led by one of the authors (P. Paronuzzi), has been based on distinct stages each with different purposes and has involved various activities, both in the field and in the laboratory, employing various investigation approaches (photo-aerial interpretation, geomorphological analysis, geological and geomechanical field survey, numerical modelling, rock and soil sampling, mineralogical and geotechnical analyses, etc.).

This articulated and time-staged research plan has led to the acquisition of a considerable amount of new information about the 1963 slope failure, including: (i) a new geological interpretation of the 1963 Vajont landslide and of the ancient (prehistoric) rock slope failures (Paronuzzi and Bolla, 2012, 2013); (ii) the first combined seepage–stability analysis aimed at examining the influence of the various filling–drawdown operations related to the Vajont reservoir (1960–1963) on the stability condition of the northern slope of Mt. Toc (Paronuzzi et al., 2013a, b); (iii) the critical re-examination of some field evidence, already noted in the past research, related to folded and sheared off rock masses possibly caused by gravity-induced processes (Paronuzzi and Bolla, 2015a, b); (iv) the overall re-analysis of the monitoring data (surface displacements, groundwater levels, microseismic recordings), which were acquired during the long period of instability that preceded the 1963 landslide, to explain the sudden and unforeseen final collapse (Paronuzzi et al., 2016). Over this comprehensive and long-term planned research work, extensive geomechanical data has been acquired both on rock and soil samples (Paronuzzi and Bolla, 2013), with particular attention devoted to the mineralogy and shear strength properties of the clays involved in the slope failure (Bolla et al., 2020).

The causes of the 1963 Vajont landslide relate to both predisposing and triggering factors. Studies by Selli and Trevisan (1964), Hendron and Patton (1985), Paronuzzi and Bolla (2012, 2015a) and Wolter et al. (2014) agree that predisposing geological factors leading to the large slope failure include: (i) the general attitude of the dip-slope bedding planes; (ii) the presence of soft clay interbeds within the thinly stratified limestone sequence of the Fonzaso Formation of Upper Jurassic age involved in the basal failure; and (iii) the presence of some major faults representing lateral and rear release surfaces. The existence of a prehistoric rockslide lying on the northern slope of Mt. Toc was also widely recognised as a determining factor for the occurrence of the 1963 Vajont slide, since the failure surface was pre-determined and the materials involved in the basal sliding would have been at or near their residual shear strength (Hendron and Patton, 1985; Kenney, 1992; Alonso and Pinyol, 2010; Paronuzzi et al., 2016). However, it must also be noted that, based on geomorphological or geotechnical considerations, some authors still dispute the occurrence of the prehistoric rockslide (Wolter et al., 2016; Dykes and Bromhead, 2018).

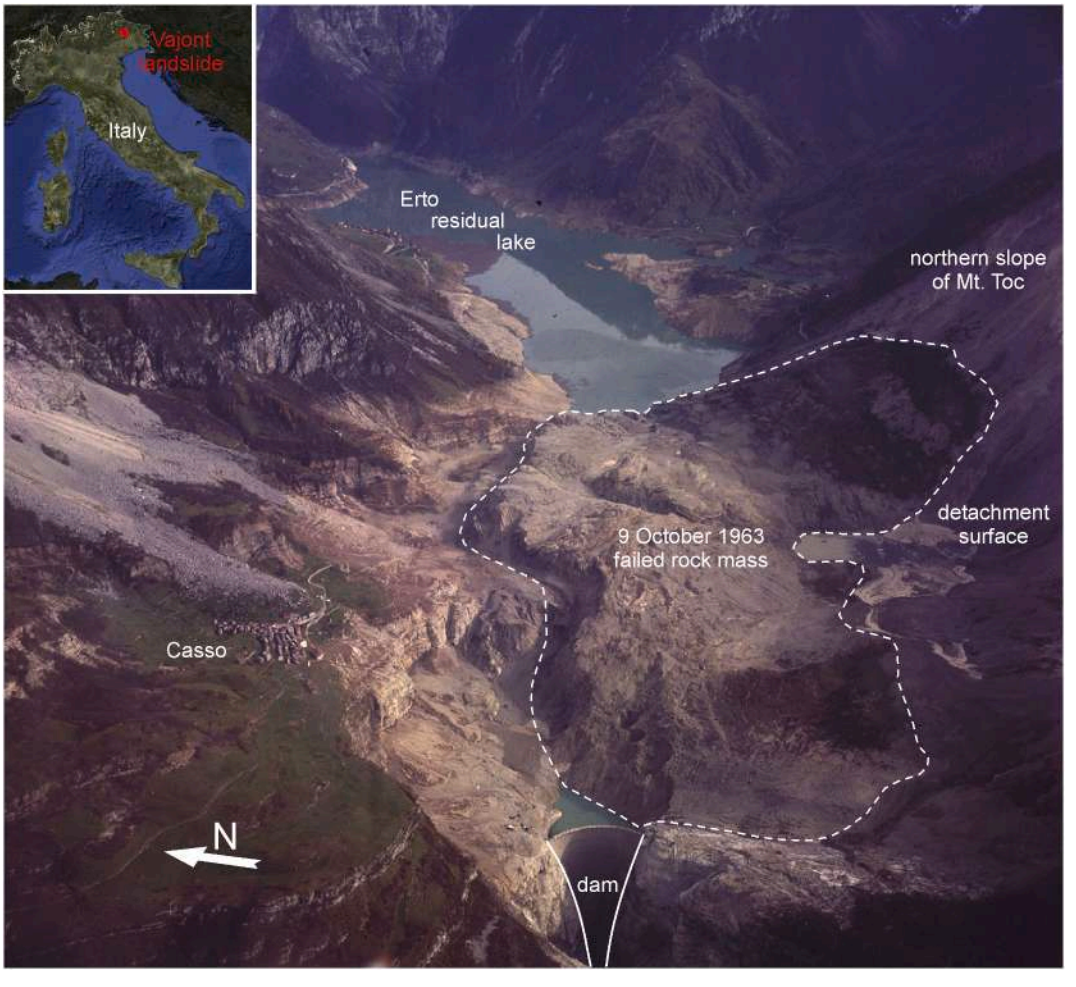

Fig. 1. Aerial view of the Vajont dam area shortly after the disaster that occurred on 9 October 1963, showing the 300 Mm^3 landslide mass that filled the artificial reservoir. This picture (available at https://www.ilpost.it/2013/10/09/il-disastro-del-vajont/vajont-dam/, Copyright holder: Associated Press Photo) was taken on 16 November 1963 and is one of the first colour pictures of the Vajont landslide after the catastrophe.

When considering other possible geological factors that favoured slope instability processes at Vajont, Skempton (1966) addressed folding of the layered sequence that gave rise to bedding plane slip occurring in weaker clayey beds, thus reducing strength to near residual values between more rigid limestone beds. Mantovani and Vita-Finzi (2003) advanced the hypothesis that the slide surface was an exhumed fault plane, with the slide material composed predominantly of fault gauge. Kiersch (1964), Müller (1968), Lo et al. (1972) and Hendron and Patton (1985) also speculated on the probable existence of artesian pressures acting along the base of the slide due to karst in the underlying oolitic limestone of the Calcare del Vajont Formation, which may have resulted in rapid rise of groundwater levels due to rainfall.

In addition, as demonstrated by extensive field evidence (Paronuzzi and Bolla, 2012, 2015a), a decisive geological factor contributing to the 1963 slide was the occurrence of a 40 m-thick shear zone at the base of the unstable slope. The basal shear zone was characterised by a chaotic assemblage of highly permeable limestone angular gravel, displaced and fractured rock masses, and spread clay lenses with high plasticity and very low residual shear strength (Paronuzzi et al., 2013a, b; Bolla et al., 2020). The debris material forming the basal shear zone was the result of the disintegration of the primary rock mass at the base of the prehistoric rockslide during the ancient slide propagation (Paronuzzi and Bolla, 2015a). The presence of this "debris cushion" at the base of the 1963 slide was extremely unfavourable for slope stability owing to the combined poor mechanical properties of clay beds and the high permeability of the limestone angular gravel, which facilitated a rapid reservoir-induced inflow. Moreover, the ductile shear zone at the base of the slide favoured the en-block motion of the 1963 catastrophic collapse (Fig. 1).

When investigating the possible triggering factor that caused the 1963 Vajont slide, studies by Müller (1964 and 1968) and Hendron and Patton (1985) gave most attention to heavy rainfalls and their distribution over the 1960–1963 period. Differently, the role played by the pore water pressure increase induced by the reservoir at the toe of Mt. Toc slope was only marginally considered or not comprehensively analysed. According to their hypothesis for the presence of an artesian aquifer beneath the main failure surface, Hendron and Patton (1985) asserted that the Vajont landslide would have occurred even in the absence of the reservoir and as a result of periods of heavy or prolonged rainfall. However, a number of borings performed after the 1963 catastrophic event never ascertained the occurrence of such an artesian aquifer in the underlying bedrock and the same is given by the current surface water flow evidence.

The first slope stability analyses that consider the variation over time of the pore water pressure caused by the fluctuations of the Vajont reservoir were only carried out recently by Paronuzzi et al. (2013, b). These combined seepage–stability analyses demonstrated that the stability condition of Mt. Toc slope was decisively controlled by the groundwater inflow induced by the reservoir level changes during the hydraulic operations performed in the period 1960–1963. Indeed, the factor of safety (FOS) of the slope greatly decreased during the three main filling stages of the reservoir (Paronuzzi et al., 2013a), thus activating the progressive failure process of localised constraints over the three-dimensional failure surface that culminated with the final slope collapse on 9 October 1963 (Paronuzzi et al., 2016). As a result, the main trigger of the 1963 Vajont landslide was the adjacent reservoir at the toe of Mt. Toc slope, which caused the formation of a water table within the highly permeable debris material of the basal shear zone, thus inducing a decrease in the overall shear strength along the failure surface (Paronuzzi et al., 2013a, 2016). At the same time, the stability analyses of the northern slope of Mt. Toc demonstrated that precipitation alone would not have led to slope collapse (Paronuzzi et al., 2013a). This means that the catastrophic 1963 slope failure could have been avoided if no reservoir had been constructed in the Vajont valley or if the reservoir level had been maintained at an elevation well below the one stipulated in the initial designed values.

Although the presence of clay interbeds within the rock mass involved in the slope rupture is considered as a determining factor in the occurrence of the catastrophic collapse, some issues still need to be addressed. In particular, the geological origin and the related provenance of the Vajont clays has never been investigated. In addition, the mechanical role played by the clay layers in both the ancient rockslide and the 1963 reactivation has not been fully understood in relation to the mineralogy, geotechnical properties, lenticular shape and lithostratigraphic position of the clay beds. These issues will be discussed in the present paper on the basis of additional geological field observations, new geochemical data on trace elements of the sampled clayey materials and further considerations on geological and mineralogical

Table 1
Mineralogical composition and values of the residual angle of internal friction of clayey materials sampled from the Vajont slide, according to different Authors.

Author (Year)	No. of samples analysed	Mineralogical composition	Residual angle of internal friction
Broili (1967)[a]	Not mentioned	8–30% clay minerals (Montmorillonite, Illite) Montmorillonite (25–75%) Illite (5–30%)	–
Kenney (1967)	3	Calcite (7–40%) Quartz (5–10%) Feldspar (0–5%)	9–16°
Nonveiller (1967)	Unknown	–	5–7°
Hendron and Patton (1985)	3	50–80% clay minerals (Montmorillonite 25–75%, Vermiculite/Smectite, Illite, Corrensite, Kaolinite), Calcite, Quartz Smectite (0–25%)	5–16°
Tika and Hutchinson (1999)	2	Illite/Smectite (25–50%) Kaolinite (<5%) Calcite (40–45%) Quartz (<10%)	9–11° (low-velocity)
Ferri et al. (2011)	1	Smectite (60–70%) Calcite (20–30%) Quartz (<5%)	24–26° at 40–60% humidity 8–10° at water saturation (low-velocity)
Bolla et al. (2020)	9	Illite/Smectite (36–96%) Calcite (4–64%) Quartz (<6%)	7–15° for clay-rich samples 20–27° for calcite-rich samples

[a] Interbeds of pelitic materials (limey marl and marly limestone).

features of the Vajont clays along with their geomechanical implications in the repeated instability processes that occurred on the northern slope of Mt. Toc.

2. Previous investigations on the Vajont clays

Despite the fact that the occurrence of clay layers within the layered sequence of the Fonzaso Formation at the base of the slide is now widely accepted, this topic was controversial for decades after the catastrophic event. As a result of the survey of the failure scar, Broili (1967) stated that the lithostratigraphic sequence involved in the rupture did not include any clay layers, although very thin 1–3 mm-thick interbeds of limey marl and marly limestone were present. X-ray diffraction analyses revealed these pelitic beds contained an average of 16% montmorillonite and probably illite clay minerals (Broili, 1967), as shown here in Table 1. However, studies by Kenney (1967) and Nonveiller (1967) reported laboratory results on the mineralogical composition and residual shear strength properties of some clay samples collected from the basal failure surface of the Vajont slide (Table 1). In particular, the first semi-quantitative determinations performed via X-ray diffraction on the Vajont clays revealed a content of 25–75% montmorillonite that resulted in low values of the residual angle of internal friction, which was found to be strongly dependant on the system chemistry (Kenney, 1967). This evidence was disputed by Müller (1968), who contended that clayey beds in the strict sense, would not be present in a limestone sequence dated to the Jurassic, inferring the presence of claystone interbeds, on the basis of Broili's (1967) interpretation. It must be noted that the lithostratigraphic sequence involved in the slope failure was not fully known at that time, and Müller's opinion was based on his knowledge of the geological aspects referred to the Jurassic age.

The debated question of clay interbeds was definitively resolved thanks to the detailed geological survey carried out on the failure surface some years later by Hendron and Patton (1985): several plastic clay layers were sampled, intercalated within the cherty limestone bedrock (Fig. 2) as well as mixed with uncemented angular gravel and sand-sized breccia forming debris strips resting on the basal detachment plane of the slide. However, the origin of this debris material was not clearly established by Hendron and Patton (1985), who supposed that it may have been the result of landslide processes (Hendron and Patton, 1985; p. 26). The clay mineral analyses pointed out the presence of 50–80% Ca-montmorillonite and some vermiculite/smectite mixed layers for the first time (Hendron and Patton, 1985; Table 1). Some residual shear strength tests on the sampled clayey materials revealed very low resistance properties, with values of the residual friction angle varying between 5° and 16°. Hendron and Patton also argued that the failure surface of the 1963 slide coincided with "one or more clay layers which were continuous over large areas of the surface of sliding" (Hendron and Patton, 1985; p. 91).

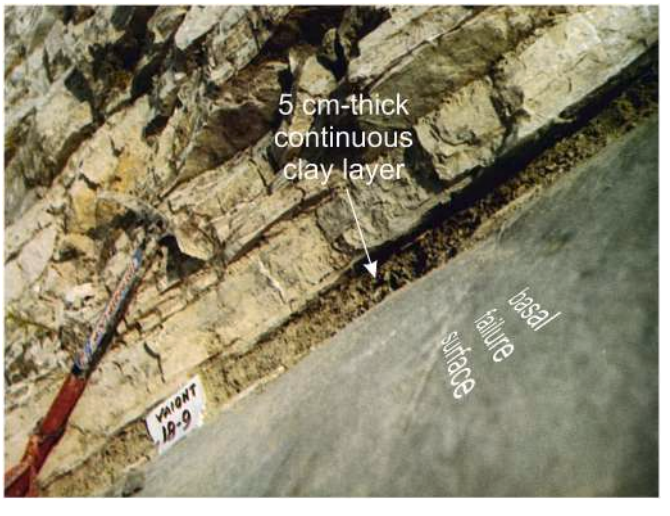

Fig. 2. Basal clay interbed as exhumed by Hendron and Patton during their field work on the failure surface; location 18–9 is close to VA15–166 of this study (photo modified from Hendron and Patton, 1985).

However, field observations carried out on the large failure surface demonstrated that the latter was not flat, and differently, was characterised by a marked stepped morphology (Broili, 1967; Paronuzzi and Bolla, 2012, 2015a; Wolter et al., 2014). In fact, the outcropping failure surface mainly follows the extended bedding planes, but also includes multiple steps coinciding with high-angle cross-cutting joints that expose different layers of the limestone sequence involved in the rupture, with directions that are both parallel and sub-orthogonal to the slide movement (Paronuzzi and Bolla, 2015a). The large extent of the exposed failure surface (about 1 km^2) is owing to its slope being close to the dip of the bedding planes, which is 34° in the western sector and 44° in the eastern sector (Paronuzzi and Bolla, 2012).

Investigations on mineralogical and strength properties of Vajont clays were also carried out in order to determine values of the friction coefficient that can explain the dynamic features of the landslide (Tika and Hutchinson, 1999; Ferri et al., 2011). In particular, Tika and Hutchinson (1999) proved the copious existence of illite/smectite mixed layers in the clay mineral mixtures occurring within the rock mass involved in the slope failure (Table 1). Ferri et al. (2011) investigated the frictional properties of a single 60–70% smectite-rich sample from the Vajont failure zone under presumably similar conditions to those during the landslide, that is using normal stresses in the range 1–5 MPa, slip rates of 2×10^{-7} to 1.31 m/s, displacements up to 34 m and variable water content from 40 to 60% up to saturation. The frictional properties of the clay-rich sample were found to decrease as strain rate and water content increased (Ferri et al., 2011).

In a recent paper (Bolla et al., 2020), mineralogical investigations of clayey materials sampled from the Vajont slide showed the occurrence of illite/smectite mixed layers as dominant clay mineral phases along with variable amounts of calcite and low quartz percentages (Table 1). The residual shear tests demonstrated, for the first time, highly variable shear resistance properties of the clay interbeds. Indeed, samples with a large prevalence of clay minerals (CM > 79%) were characterised by low values of the residual angle of internal friction (7–15°), whereas clayey materials characterised by a higher content of granular minerals (calcite and quartz) showed greater values of the residual friction angle (20–27°).

3. Materials and methods

3.1. Fieldwork and sampling

Previous field surveys performed by the Authors on the 1963 Vajont slide were aimed at identifying and sampling clayey materials occurring within the rock mass involved in the slope failure (Paronuzzi and Bolla, 2012, 2013, 2015a). Bolla et al. (2020) subsequently reported the first results of laboratory investigations of the chemical and mineralogical composition of the Vajont clays, which was determined through major oxide X-ray Fluorescence (XRF) and semi-quantitative X-ray Powder Diffraction (XRPD) analyses, along with their geotechnical properties. In the present paper, a more detailed analysis of the geochemical and mineralogical characteristics of the Vajont clays will be presented and discussed, along with new laboratory investigations and additional field observations.

Clay samples were collected from both the northern side of the Vajont valley, where the lithostratigraphic sequence is better exposed, and the failure surface of the 1963 Vajont landslide (for the sampling location, see Fig. 3). Field evidence includes the identification of the different geological contexts in which the clay layers occur. Particular attention was paid to the specific stratigraphical situation of the clay interbeds within the limestone sequence involved in the slope failure.

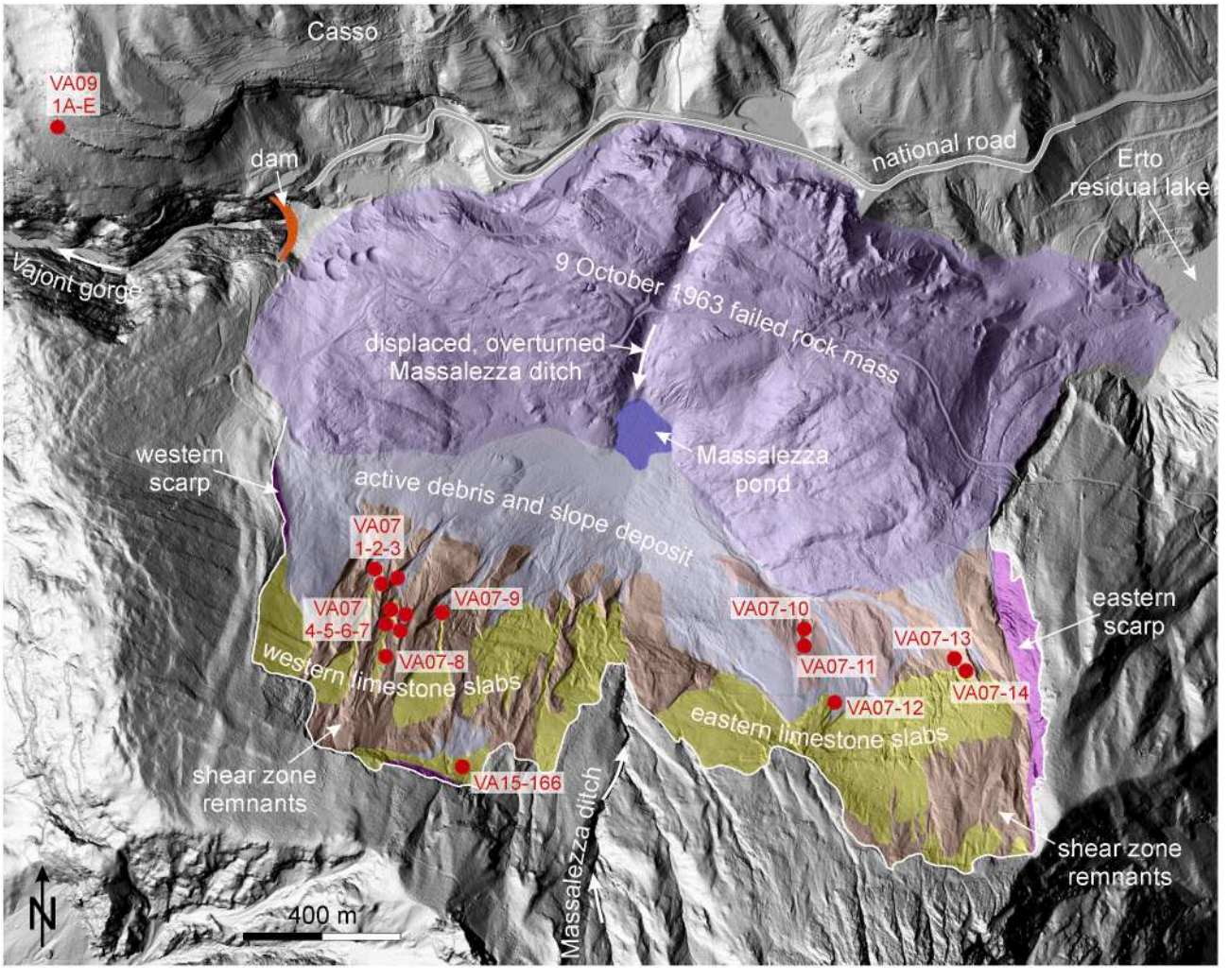

Fig. 3. Shaded relief map of the 1963 Vajont landslide and its surroundings showing the remnants of the basal shear zone resting on the detachment surface, along with the locations and identification numbers of the clay samples.

Some relevant outcrops were cleaned, pointing out the stratigraphical contacts, and coded, photographed and drawn. The outcrops of clayey materials were accurately prepared before the sampling procedure: the surface debris and the soil cover were always removed, thus avoiding or limiting possible physical (e.g., induration) and/or mineralogical changes caused by weathering processes. The clays were generally found in an unweathered condition. Additional observations were acquired on the stepped morphology of the basal rupture surface exposed on the slide failure scar. The newly acquired geological data allowed us to reconstruct the two updated lithostratigraphic columns referring to both sides of the Vajont valley (Fig. 4).

3.2. Mineralogy and chemistry

The mineralogy of the sampled clays was investigated in more detail here, specifically as regards the characterisation of illite/smectite (I/S) interstratifications, according to the criteria illustrated in Moore and Reynolds Jr. (1997). The degree of ordering between illite and smectite in mixed layers, that is the Reichweite *R*-type and illite percentage (%I) in I/S mixed layers was determined for each sample. Calcimetric analyses were performed on the sampled clayey materials in order to determine the content of calcium carbonate by using a "De Astis" calcimeter at a temperature of 20 °C. The analyses were performed at the Chemical Laboratory of the Department of Physical Sciences, Earth and Environment of the University of Siena (Italy).

Trace element geochemical data was determined through X-ray fluorescence analyses that were performed via a WDS sequential Philips PW2400 spectrometer at the Department of Geosciences of the University of Padua (Italy). The analyses were performed on glass bead samples (1:10 ratio with flux $Li_2B_4O_7$). For the determination of the trace elements, precision is within 3% and detection limits are: 10 ppm for Ba, La, Ce and Nd; 6 ppm for Cr; 5 ppm for V, Ga and Pb; 3 ppm for Co, Ni, Cu, Zn, Rb, Sr, Y, Zr, Nb, Th and U.

4. The clays involved in the Vajont landslide

4.1. Field characterisation

The lithostratigraphical sequence occurring along the final stretch of the Vajont valley includes a complex limestone sequence dating from Middle Jurassic to Upper Cretaceous that is almost entirely exposed on the northern valley side, near the village of Casso. The outcropping geological formations (Fm.) are the following, from the bottom to the top ("Casso sequence" in Fig. 4):

- Calcare del Vajont (OOV);
- Fonzaso (FOZ);
- Ammonitico Rosso Veronese Superiore (ARV_3);
- Maiolica (MAI);

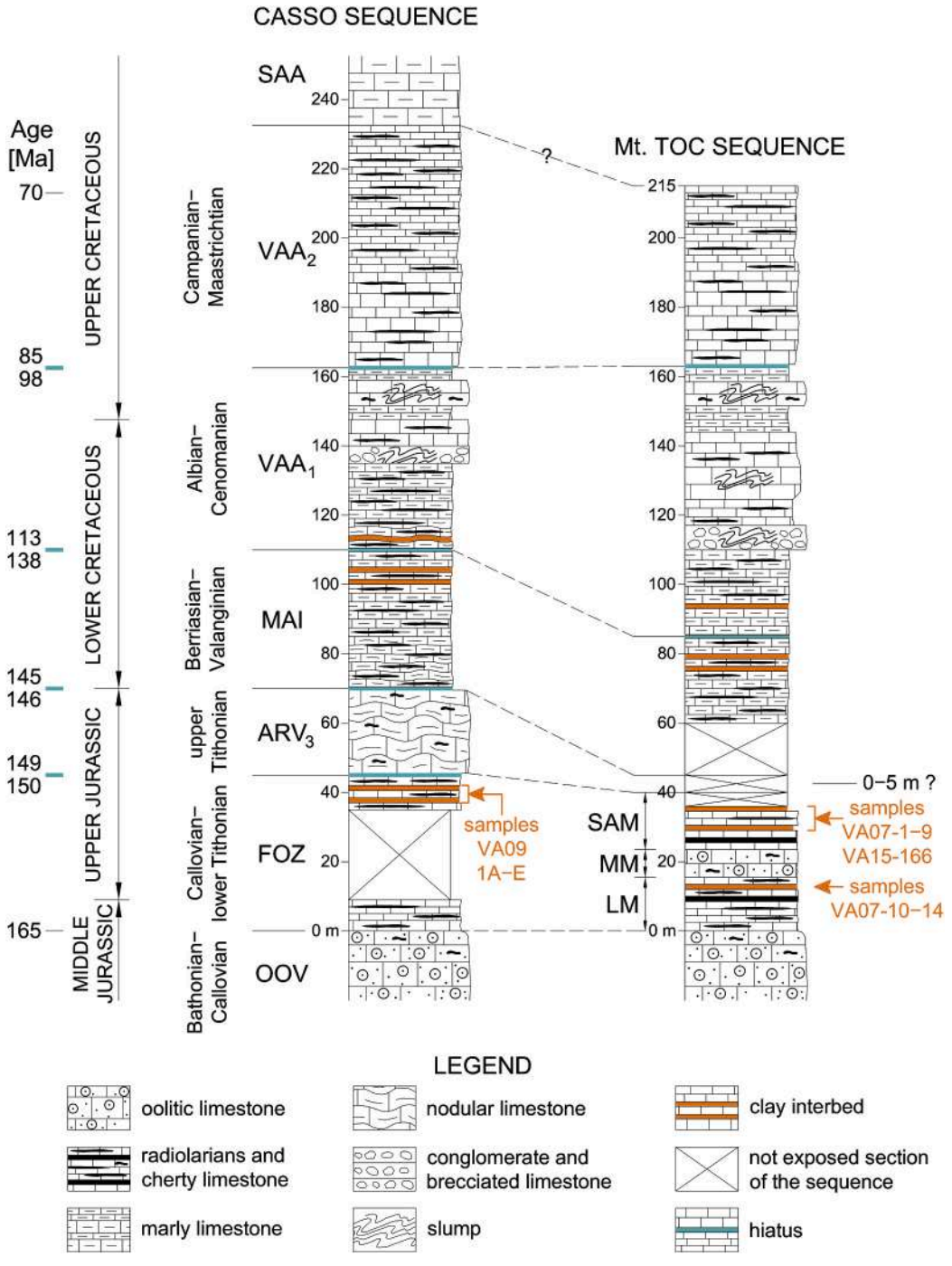

Fig. 4. Lithostratigraphic columns of both sides of the Vajont valley. The locations and identification numbers of the clay samples are as shown.

- Scaglia Variegata Alpina (lower member VAA_1 and upper member VAA_2); and
- Scaglia Rossa Friulana (SAA).

On the northern slope of Mt. Toc (southern valley side), the lithostratigraphic sequence that was involved in the 1963 Vajont landslide ("Mt. Toc sequence" in Fig. 4) has some differences if compared with the Casso sequence, since it does not include the overlying Scaglia Rossa Friulana Fm., and exhibits variable thicknesses of some geological formations, in particular of ARV_3. A part of the Jurassic–Cretaceous sequence was involved in the formation of the shear zone at the base of the Vajont landslide (Paronuzzi and Bolla, 2012, 2013), which formed as a result of the prehistoric Mt. Toc rockslide that occurred in the Late Pleistocene–early Holocene period (Paronuzzi and Bolla, 2015a). The geological formations included in the shear zone are, from the bottom to the top: the upper two thirds of FOZ, ARV_3, MAI, and the first 10–15 m of VAA_1 (Fig. 4).

The basal failure surface of the slide mainly coincides with the bedding planes of the 5–10 cm-thick cherty limestone layers of the Fonzaso Fm. Borehole data acquired from drilling of the bedrock performed after the 1963 landslide on the western border of the detachment surface (borehole R7; see Martinis, 1978) shows that the basal failure plane there is located about 25 m above the stratigraphic contact with the underlying OOV. Unfortunately, no borehole data exists for the bedrock stratigraphy on the eastern part of the detachment surface.

The Fonzaso Fm. includes several clay interbeds of variable

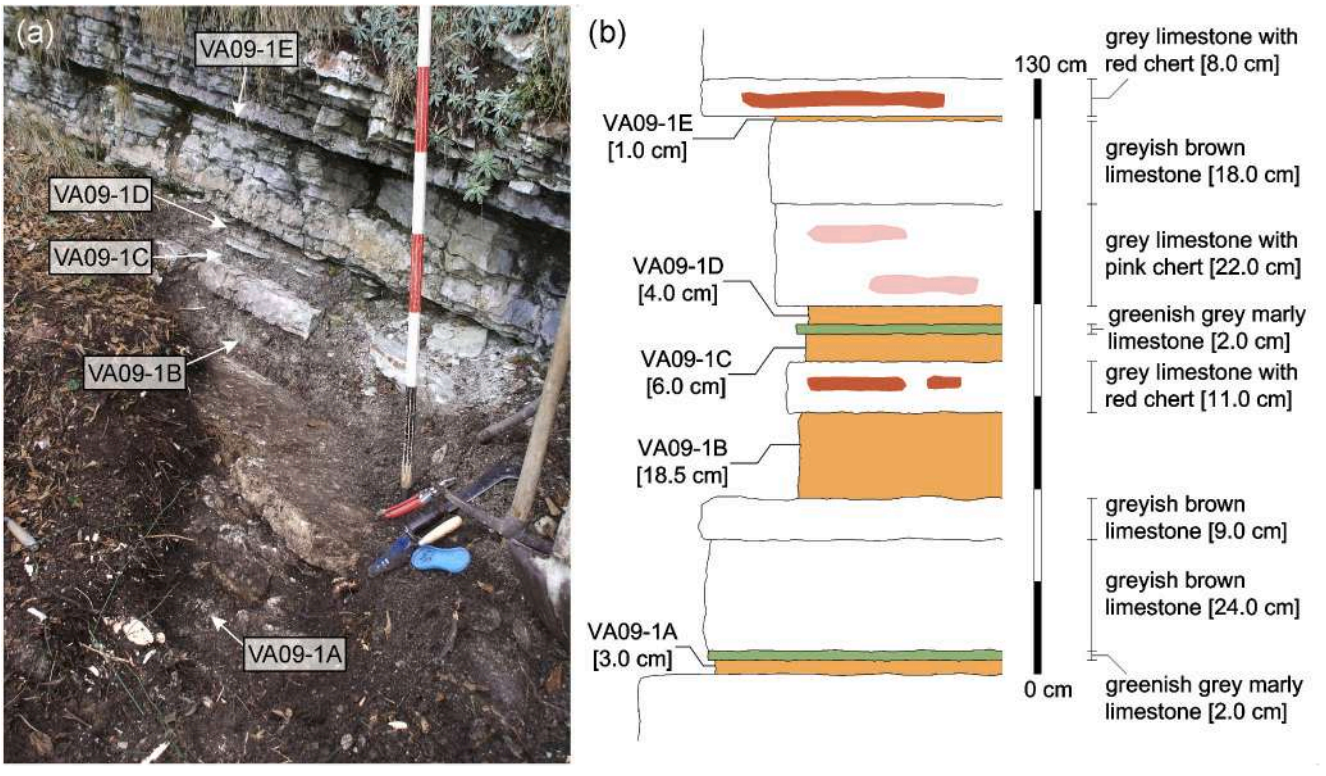

Fig. 5. (a) Rock outcrop (top of the Fonzaso Fm.) on the north valley side from which 5 clay layers were sampled, and (b) its schematisation. For the sampling location see Fig. 3.

thicknesses, from 0.5 cm to 6 cm in most cases, but some layers up to about 20 cm-thick occur in the Casso stratigraphic sequence. The clay interbeds are not evenly distributed within the whole 40–45 m-thick Fonzaso Fm. In fact, the lowest 10–15 m stratigraphic beds of FOZ (lower half of the Listato Member, LM) do not include any clay layers (Fig. 4), as visible near the Vajont dam, where the stratigraphic contact between OOV and FOZ is clearly exposed. On the contrary, frequent clay interbeds characterise the upper sequence of the Fonzaso Fm. (30–40 m, that is at the top of the Scisti ad Aptici member, SAM; Fig. 4). Several 1.0–18.5 cm-thick clay layers were observed in a rock outcrop located on the north valley side, to the west of the village of Casso (Figs. 3, 5a), at the stratigraphic contact between FOZ and the overlying ARV_3.

This small rock scarp is the same outcrop studied by Hendron and Patton (1985) during their field investigations (outcrop 8–1, see Photos 1–3 and Fig. 14 in Hendron and Patton, 1985). The 130 cm-thick sequence includes five greyish and yellowish clay layers (VA09–1A–E) interbedded with layers of grey cherty limestone and greenish marly limestone (Fig. 5b). These clay layers extend laterally about 10–15 m. The clay interbed coded as VA09–1B is the thickest layer ever surveyed in the Vajont valley. This outcrop is particularly important since it provides field evidence that multiple clay layers are concentrated within certain parts of the limestone sequence. As shown in Fig. 5, five 1 to 18.5 cm-thick clay interbeds occur in a 1.3 m-thick sequence of cherty limestone layers.

The basal rupture surface exposed on the failure scar of the 1963 Vajont landslide (western and eastern limestone slabs in Fig. 3) has a marked stepped morphology (Wolter et al., 2014; Paronuzzi and Bolla, 2015a). Two orders of rock steps can be identified, on the basis of their strike compared with the dip direction of the stratification joints, which is close to the main sliding direction (Fig. 6). Lateral steps occur in directions that are sub-parallel or oblique to the dip direction of the rock strata, whereas transverse steps occur sub-orthogonally to the latter (Fig. 6a, b). Most lateral steps are 1–5 m-high (Fig. 6c) and coincide with large tectonic fractures or pre-existing macro-joints (Paronuzzi and Bolla, 2015a). On the other hand, as demonstrated in Fig. 6d, the transverse steps are smaller and exploit newly formed fractures related to the slope progressive failure (i.e., gravity-induced joints; Paronuzzi and Bolla, 2015b) within a single 5 to 10 cm-thick limestone layer or a series of beds between 0.5 and 1 m-thick.

These steps form rock scarps that expose different parts of the bedrock beneath the basal sliding surface. When considering all these steps, a total thickness of about 15–20 m of the FOZ sequence is exposed on the large failure scar of the slide. Interestingly, clay interbeds within the in-situ limestone sequence outcropping on the detachment surface are very rare, since only one clay layer was therein identified during the field surveys (VA15–166 in Figs. 3 and 6b). This clay layer is located very close to the clay interbed exhumed by Hendron and Patton (1985) and shown in Fig. 2.

Remnants, up to 10–12 m-thick, of the primary shear zone are visible in several outcrops on the western and eastern basal shear surfaces (Fig. 3). The shear zone material includes limestone angular gravel that underlies or completely surrounds large blocks of strongly fractured and folded stratified rock masses (Paronuzzi and Bolla, 2012). Clayey materials were identified in different geological contexts related to the basal shear zone of the Vajont slide (Fig. 7): clay layers occur as lenses or interbeds (i) at the basal failure surface (Fig. 7a, b), (ii) within the displaced stratified rock masses (Fig. 7c, d), or (iii) they are mixed with the limestone angular gravel (Fig. 7e, f).

Clay lenses occurring on the basal sliding surface are commonly characterised by a thickness of 3–7 cm. Differently, the clay layers included in the stratified rock masses are isolated 0.5 to 2 cm-thick lenses or interbeds of grey, greenish, and yellowish clay. However, most of the clay layers identified on the field are included in the limestone angular fragments originated by the disintegration of the rock strata. In some circumstances, 1 to 4 cm-thick clay layers of variable colours appear as spread, contorted and discontinuous lenses. In many cases, multiple and overlying clay lenses are concentrated in 1 to 2 m-thick debris strips. Field observations also ascertained that, in any case, the

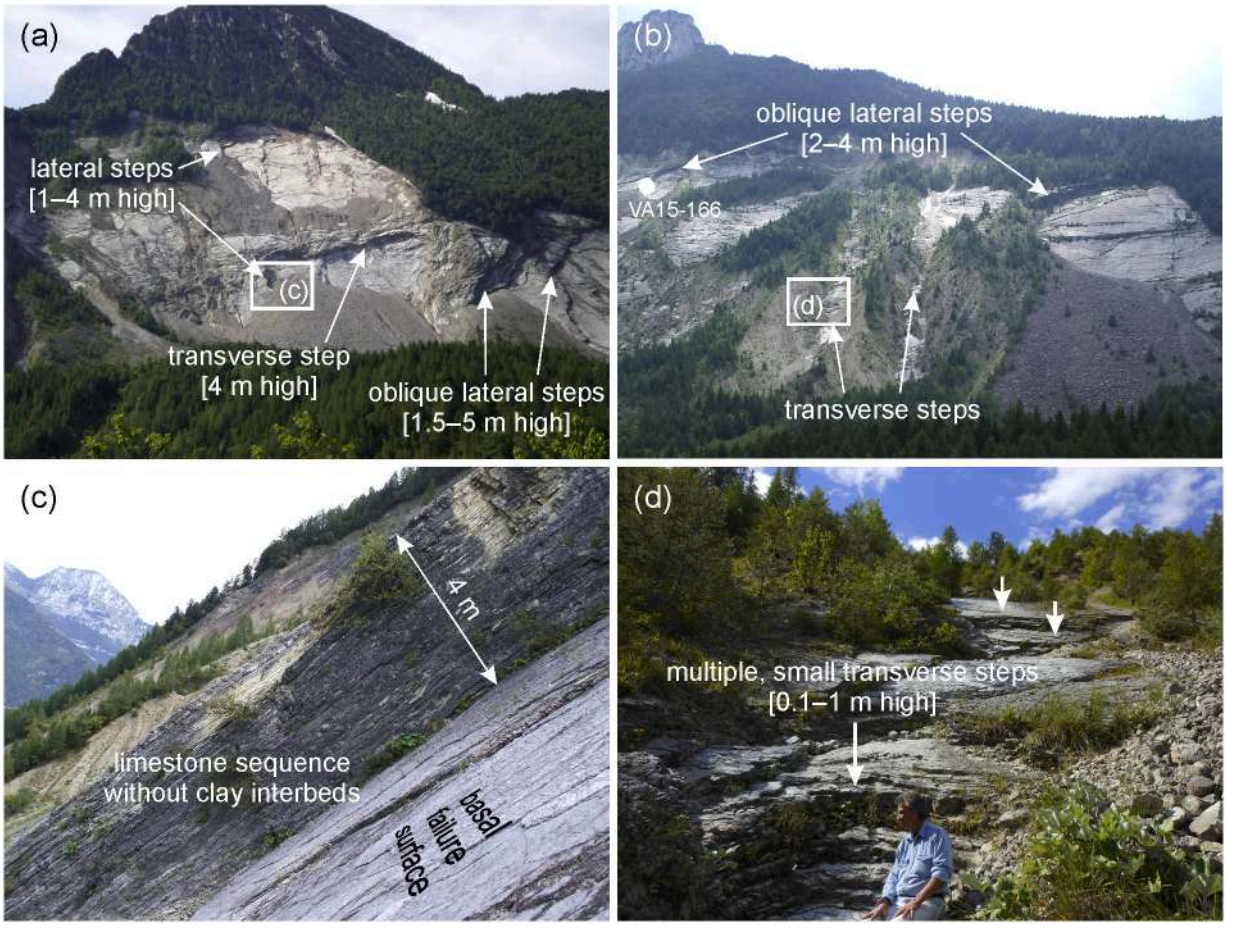

Fig. 6. Stepped morphology of the basal failure surface characterising (a) the eastern part and (b) the western part of the detachment surface of the Vajont landslide. (c), (d) Details of a lateral step and multiple transverse steps, respectively, showing the in-situ lithostratigraphic sequence outcropping on the failure surface (Fonzaso Fm.).

clay lenses have continuity lower than 10–15 m.

4.2. Mineralogical and geochemical characterisation

XRPD analyses reported by Bolla et al. (2020) showed that the clay layers consisted mainly of clay minerals, calcite and quartz (Table 2). Semi-quantitative estimation of clay and non-clay minerals was performed on bulk samples by measuring peak areas in the diffractograms of each phase, as described in Bolla et al. (2020). When referring to clay minerals, the detailed analysis of air-dried, heated and ethylene glycolated oriented mounts performed on the <2 μm fraction showed the almost exclusive occurrence of illite/smectite (I/S) mixed layers in all the investigated sediments. Other minerals occurring in some samples as traces only were: K-feldspar, kaolinite, illite and probably chlorite (Table 2).

However, a very complex admixture of I/S with different illite contents and degrees of ordering was outlined in different samples. In particular, samples VA07–3A, VA07–3B, VA07–8, VA09–1A and VA09–1B showed a prevalence of I/S mixed layers with *R*0 stacking order (50–60% illite layers) and subordinate I/S of the *R*1 type with a variable illite content (Table 2). The remaining samples were characterised by a prevalence of the *R*1 stacking order with a variable illite content. In detail, samples VA07-5A and VA07-11A were characterised by both *R*1 and *R*0 stacking orders with I% ~ 60–70% and I% ~ 50%, respectively; whereas samples VA07-13C and VA07–14 showed almost exclusively I/S *R*1 with about 70–80% of illite (Table 2).

According to the semi-quantitative estimation of the mineral content for each investigated sample, two well-defined groups of samples were distinguished (Bolla et al., 2020; Table 2). Samples VA07–3A, VA09–1A, VA09–1B, VA07-11A (Fig. 8a, b), VA07-13C and VA07–14 showed a large amount of clay minerals, from 79% up to 96%; whereas samples VA07–3B (Fig. 8c, d), VA07–8 and VA07-5A were characterised by a higher content of calcite, from 34% to 64% (Fig. 9a). Amounts of quartz did not exceed 6% in the investigated samples. Calcite contents determined through the semi-quantitative estimation were always slightly lower than corresponding $CaCO_3$ percentages that were obtained by means of the calcimetric analyses (Table 2). However, the average difference between the two data sets was 4.8%, which represents quite a good agreement.

Major oxide geochemical data (see Table 1 in Bolla et al., 2020) correlates well with the amounts of clay minerals and calcite occurring within the analysed samples. In fact, the contents of SiO_2, Al_2O_3 and K_2O were, on average, higher for clay-rich samples and lower for calcite-rich samples. On the contrary, loss on ignition (LOI) and the content of CaO were higher for calcite-rich samples and lower for clay-rich samples. This means that SiO_2, Al_2O_3 and K_2O were strictly correlated with the I/S mixed layers, as expected, whereas CaO was mainly associated with calcite.

Table 3 shows the trace element geochemical data for the Vajont clays. The average content of Zr, Zn, Ba and Ni was higher than 100 ppm, Cu, Rb and Sr were in the range 50–100 ppm, V, Co, Ga, Y, La, Ce, Nd, Pb and Th were within 10 and 50 ppm. Chromium, Nb and U were below 10 ppm. The content of some trace elements was found to be strongly dependent on the mineralogical composition of the analysed samples, since these elements were strictly associated with clay minerals rather than other minerals (or colloids) occurring in the sampled soils. For

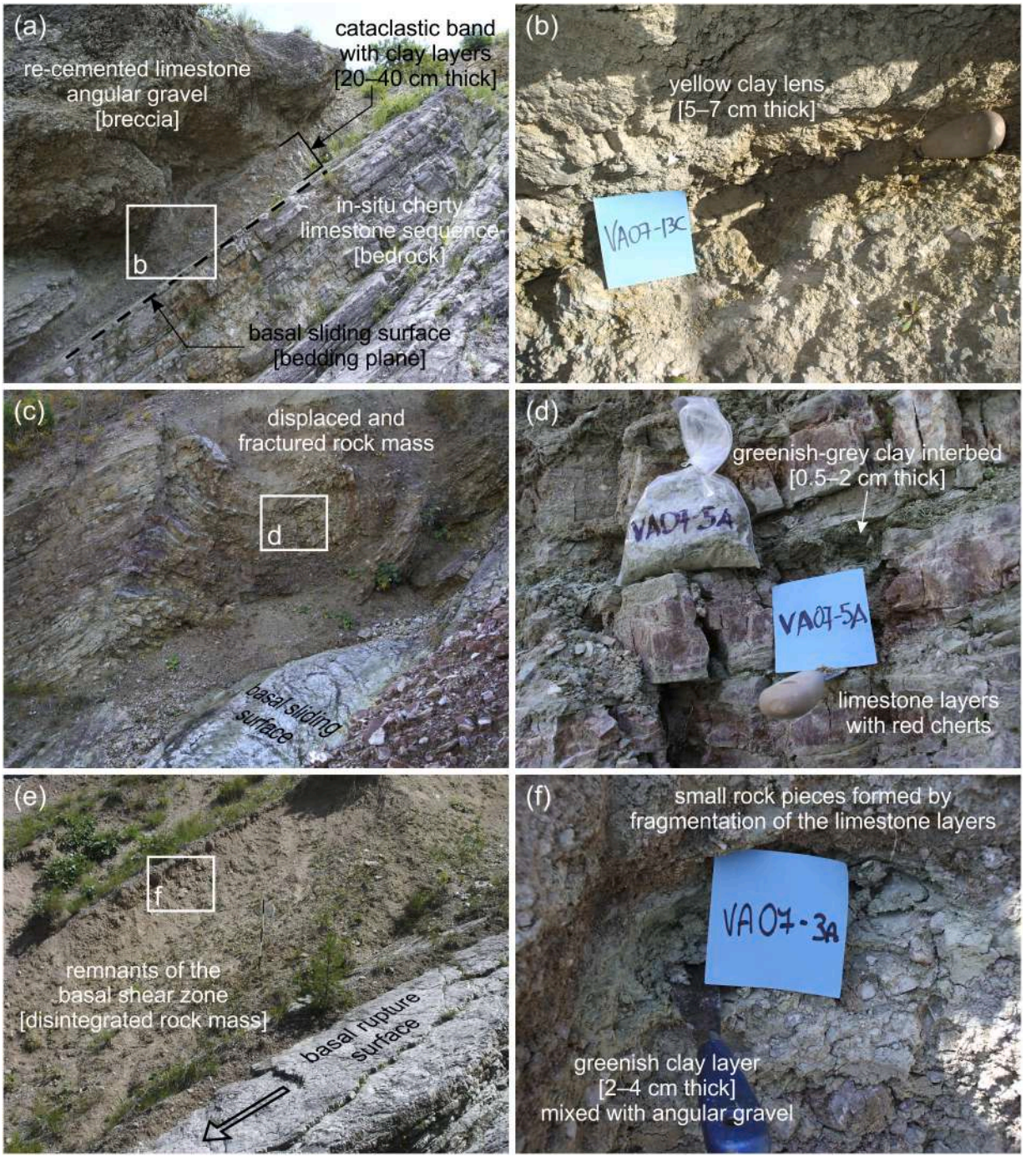

Fig. 7. Clayey materials involved in the 1963 Vajont landslide and occurring: (a), (b) at the basal contact with the sliding surface; (c), (d) within a displaced and stratified rock mass; and (e), (f) within the debris of the landslide shear zone. Sample locations shown in Fig. 3.

example, V, Sr, Y, La, and Nd were at their highest for calcite-rich sample VA07-5A and at their lowest for clay-rich sample VA07–14; whereas the opposite (i.e., lowest vs. highest) was observed for trace elements Ga and Zr occurring in the same samples (Table 3).

5. Genesis and provenance of the Vajont clays

5.1. The Vajont K-bentonites

All the Vajont clay samples showed a very similar mineralogical composition and geochemical fingerprint. The dominant clay minerals were I/S mixed layers with a 85–50% content of illite layers, thus predominating over smectite (Table 2). This is consistent with the geochemical data in that a significant percentage of K_2O (1.17–5.77%) was present in the sampled clays (see Table 1 in Bolla et al., 2020). Smectite-rich clays were identified in many rock mass sequences of various geological ages thanks to detailed lithostratigraphic analyses that allowed for the recognition of very thin layers of clays (mm- or cm-thick), often with high-plasticity properties, interbedded within various rock strata sequences (Huff, 2016 and references therein). Those particular clays were interpreted as deposits of volcanoclastic materials (tephra), sometimes altered by hydrothermal processes or by diagenesis, representing key stratigraphic levels that are very useful for chronological correlations of different lithostratigraphic sequences

Table 2
Geological context, mineralogical composition and calcite content of selected clay samples (< 2 μm fraction) from Vajont (modified from Bolla et al., 2020).

Sample	Geological context	Reichweite[d]	Illite percentage[d]	Clay minerals[e]	Calcite[e]	Quartz[e]	$CaCO_3$ from calcimetry
				[wt%]	[wt%]	[wt%]	[wt%]
VA07–3A[a]	Disintegrated rock mass	*R*0, *R*1	50–60%, 60–70%	83	17	< 1	29
VA07–3B	Disintegrated rock mass	*R*0, *R*1	n.d.	59	39	3	43
VA07–8[a]	Disintegrated rock mass	*R*0, *R*1	50–60%, 70–80%	60	34	6	41
VA09–1A	In-situ sequence	*R*0, *R*1	50–60%, 80–85%	79	19	2	19
VA09–1B	In-situ sequence	*R*0, *R*1	50–60%, 80–85%	89	10	1	18
VA07-5A[b]	Displaced rock mass	*R*1, *R*0	60–70% and 80–85%, 50%	36	64	< 1	66
VA07-11A	Displaced rock mass	*R*1, *R*0	60–70%, 50%	90	9	1	12
VA07-13C	Basal contact	*R*1	70–80%	79	17	4	23
VA07–14[c]	Basal contact	*R*1	70–80%	96	4	0	5

[a] Kaolinite and illite as traces (not determined).
[b] Kaolinite as traces (not determined).
[c] Feldspars as traces (not determined).
[d] Determined according to the criteria described in Moore and Reynolds Jr. (1997)
[e] Estimated by measuring peak areas in the diffractograms, as described in Bolla et al. (2020).

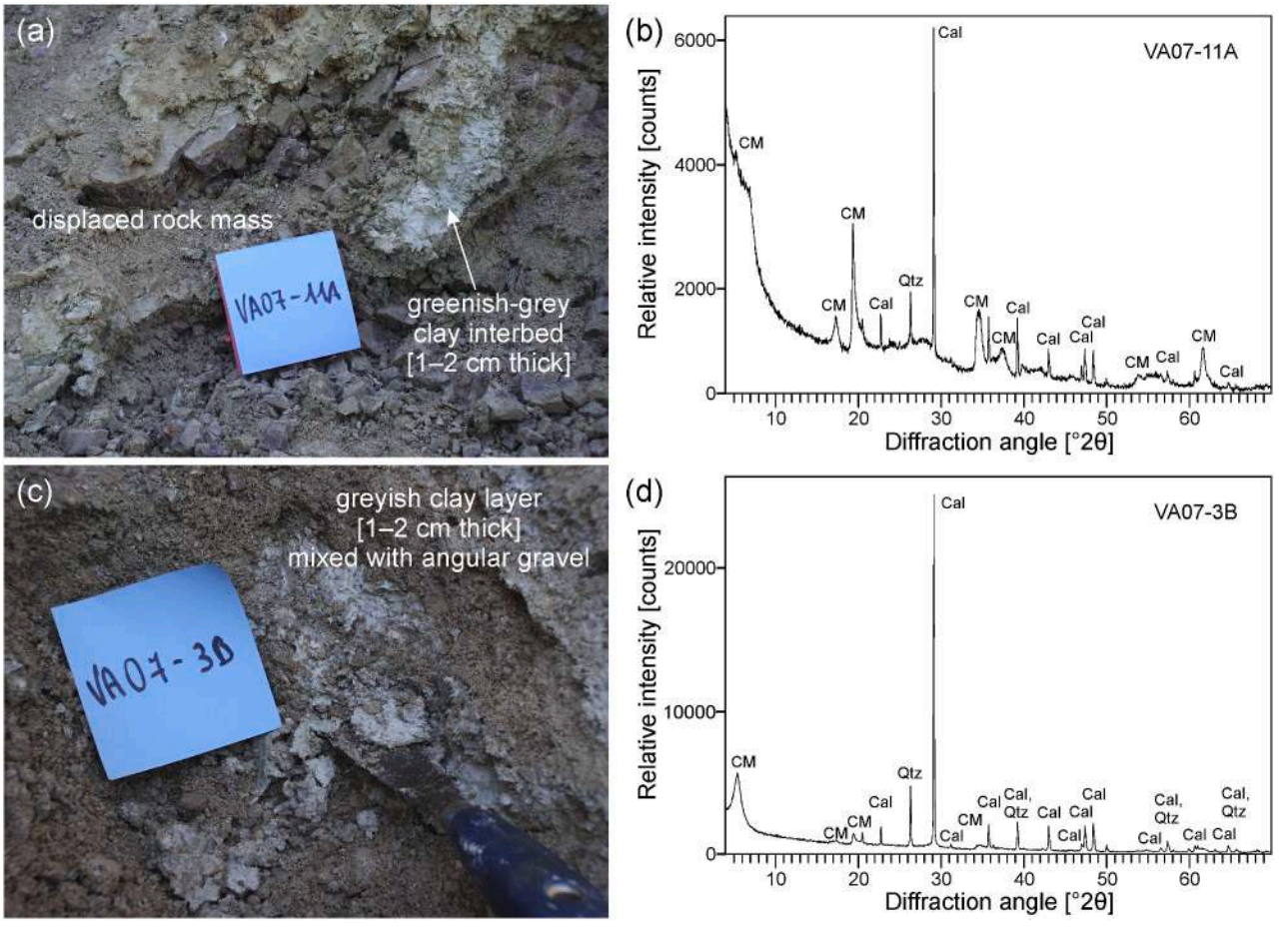

Fig. 8. Field sampling and XRPD patterns of (a)-(b) clay-rich sample VA07-11A, and (c)-(d) calcite-rich sample VA07–3B. For the sample locations see Fig. 3.

(tephrochronology). Smectite-rich clays were also indicated as bentonites or K-bentonites (Huff, 2016), depending on the percentage of potassium that is accounted for by illite. Mineralogical and geochemical data shown in the present study indicates that the Vajont clays included in the Fonzaso Fm. can be described as K-bentonites, considering the high percentage of illite that was identified in the I/S mixed layer clays.

The bentonites of the Vajont valley can be interpreted as distinct tephra levels, i.e. repeated volcanoclastic events causing sedimentary inputs of volcanic ashes that interrupted the "normal" calcareous sedimentation within this small Jurassic basin at the easternmost boundary of the Belluno Trough. Stratigraphic field evidence highlights the occurrence of several mm- or cm-thick clay layers alternated with 5–10 cm-thick platy cherty limestone beds, often occurring as 3–5 distinct layers within a 1–2 m-thick rock sequence (Fig. 5). This evidence demonstrates that explosive volcanic events occurred with a certain frequency during the Upper Jurassic, originating multiple tephra levels.

K-bentonites of the Fonzaso Fm. exhibited rather constant geochemical and mineralogical characteristics (dominance of I/S mixed layers), for both the tephra involved in the basal rupture of the Vajont landslide and those sampled within the in-situ lithostratigraphic

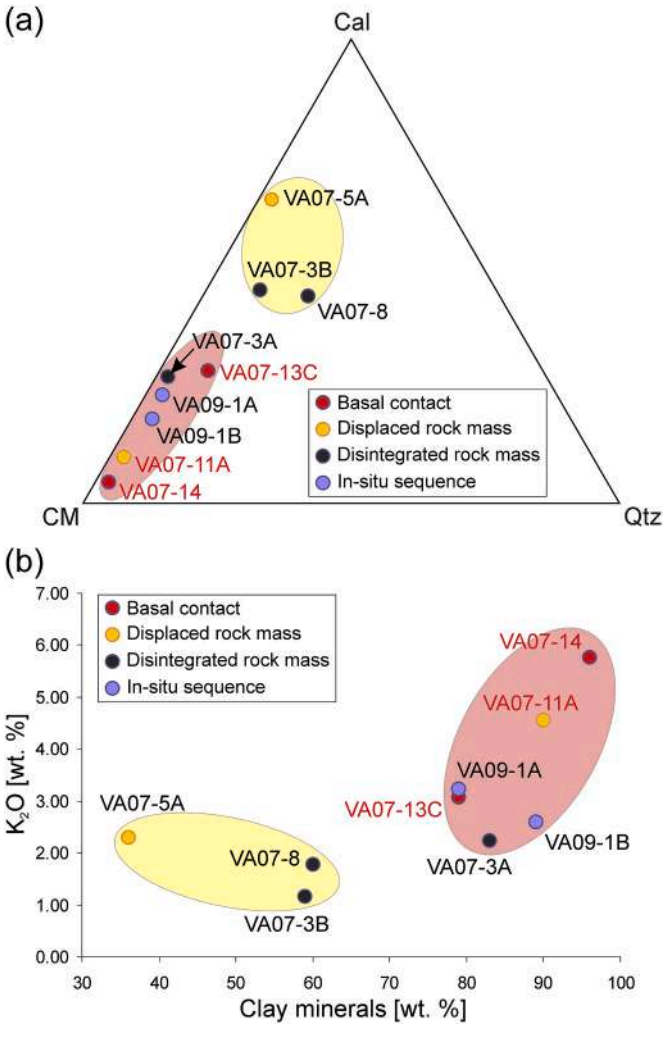

Fig. 9. (a) Ternary diagram showing the relative amount of clay minerals (CM), calcite (Cal) and quartz (Qtz) within the studied samples. (b) Diagram showing the relationship between the amount of clay minerals and K_2O content of the Vajont clays. Samples with red labels were collected from the eastern detachment surface, whereas samples with black labels come from the western part of the failure scar. (For interpretation of the references to colour in this figure legend, the reader is referred to the web version of this article.)

sequence outcropping near the village of Casso on the northern side of the Vajont valley. This fact emphasises a strong mineralogical similarity between the K-bentonites sampled within the two sedimentary sequences, suggesting the same volcanic source and also a comparable geological age: the possible maximum difference in age between the two tephra sequences is in the order of 0.1–0.3 to 1–3 Ma. When considering the whole lithostratigraphic sequence (Fig. 4), the tephra levels of the Fonzaso Fm., in absence of specific biostratigraphic studies or absolute dating, could tentatively be attributed to the late Oxfordian–upper Tithonian, and an age within the time span 158–145 Ma seems to be the most probable (Luca Martire, personal communication). This is the first recognition of bentonitic layers within the Upper Jurassic Fonzaso Fm., that is a typical cherty limestone sequence characterising the larger Belluno Basin located westward to the Vajont valley.

5.2. Genesis of the I/S mixed layer clays

I/S mixed layers with different percentages of illite commonly occur in ancient bentonites of various ages (Huff, 2016 and references therein). According to a widespread literature (Bethke et al., 1986; Cuadros and Altaner, 1998; Inoue et al., 2005), these minerals are intermediate members of the progressive reaction of smectite-to-illite conversion known as smectite "illitization", which occurs as the result of diagenetic or hydrothermal processes. Temperature is considered the main factor controlling this transition (Merriman and Peacor, 1999; Árkai, 2002; Merriman, 2005; and reference therein), although other variables such as time (Pytte and Reynolds, 1989), availability of K (e.g. Huang et al., 1993; Weibel, 1999) and fluid circulation (Eslinger and Pevear, 1988) may also significantly influence the process. According to a diagenetic origin, the illite content and ordering of illite/smectite, from random I/S (*R*0 with S > 50%; Moore and Reynolds Jr., 1997) up to ordered I/S (*R*1 and *R*3 with *I* > 50%; Moore and Reynolds Jr., 1997), are commonly interpreted as indicators of degree of burial diagenesis.

In contrast to previous descriptions, Lanson et al. (2009) described a two-stage process of smectite illitization. The early stage is characterised by the coexistence of discrete smectite and randomly, illite-rich (I > 50%) I/S interstratified clay. With increasing burial depth, they found an increase in the relative proportions of I/S, essentially at the expense of discrete smectite, with a slightly more illitic composition in the I/S mixed layers. In the second stage of smectite illitization, two illite-containing mixed layers were observed (Lanson et al., 2009). According to Fang et al. (2017), the smectite illitization of volcanoclastic bentonites may also be the result of microbial activities that induce dissolution and precipitation processes.

If we consider the widely accepted diagenetic theory as the main process causing the smectite illitization of the Vajont clay interbeds, a low diagenetic maturity is generally suggested in most of the investigated samples (VA07–3A, VA07–3B, VA07–8, VA09–1A and VA09–1B) owing to the occurrence of appreciable amounts of I/S *R*0 ordering type and an illite content of around 50%. The concurrent presence of I/S *R*1 with higher illite percentages in the same samples suggests that these minerals may have been derived from the neighbouring area at the time of deposition.

The occurrence of a prevailing or exclusive *R*1 ordering type with high illite contents in the other samples (VA07-5A, VA07-11A, VA07-13C and VA07–14) may suggest a higher diagenetic maturity, but further evidence is necessary to validate this hypothesis. Interestingly, a

Table 3
Content of trace elements (parts-per-million) from XRF analysis of selected Vajont clay samples.

Sample	Elements [ppm]																		
	V	Cr	Co	Ni	Cu	Zn	Ga	Rb	Sr	Y	Zr	Nb	Ba	La	Ce	Nd	Pb	Th	U
VA07–3A	14	<6	16	78	44	122	21	47	156	16	114	7	104	24	39	43	44	30	6
VA07–3B	16	13	14	58	41	81	20	33	117	20	77	14	83	13	32	41	42	28	< 3
VA07-5A	25	8	22	129	109	145	13	79	198	47	78	4	199	42	33	51	22	25	5
VA07–6	8	< 6	19	81	109	125	24	63	73	18	261	8	137	11	19	44	48	13	8
VA07–8	15	< 6	17	64	39	100	17	51	89	24	78	13	118	34	47	44	47	23	< 3
VA07-11A	< 5	8	24	181	76	221	26	102	78	12	232	4	147	< 10	14	35	40	15	6
VA07-13C	18	< 6	22	123	65	179	25	111	46	15	147	7	142	18	27	38	44	26	7
VA07–14	< 5	6	7	101	53	153	28	134	27	15	270	5	135	< 10	< 10	30	28	17	7
VA09–1A	24	< 6	39	123	88	158	24	80	43	25	228	9	88	< 10	< 10	35	33	17	6
VA09–1B	6	< 6	38	222	42	162	29	56	37	9	106	18	56	37	37	35	80	34	7

prevailing I/S *R*1 type occurred in clay samples that were acquired from the eastern limestone slabs outcropping on the detachment surface of the slide, whereas the I/S *R*0 mixed layer minerals were mainly associated with clay layers sampled from the western limestone slabs and from the in-situ lithostratigraphic sequence outcropping near the village of Casso (Figs. 3 and 4 and Table 2). However, a more detailed correlation between the different lithostratigraphic sequences outcropping on the failure scar needs a further investigation, for instance by means of biostratigraphic data.

When considering the genesis of the I/S mixed layers of the investigated sediments, it is also necessary to examine the possible origin of the primary smectite minerals occurring in the tephra levels that were further included in the Vajont clay interbeds. The formation of smectite minerals is very often related to volcanic rocks, both mafic and felsic rocks, and volcanoclastic sediments. However, the suggested formation process for smectites in volcanoclastic deposits can be very variable and includes: (i) the hydrothermal origin caused by the alteration of volcanic glass particles (Fiore, 1993; Mirabella et al., 2005) or by the precipitation from fluids that are mixtures of magmatic and local meteoric water located within volcanic vents (Mizota and Faure, 1998); (ii) the deuteric alteration, i.e. a low-temperature magmatic alteration related to the solidification of a melt (Spinola et al., 2017); and (iii) the weathering of volcanic ashes during the early stages of diagenesis at the sediment/seawater interface (Pellenard et al., 2013).

The latter formation process is generally assumed for most of the bentonite deposits in which the middle alkalinity of marine environment favoured the alteration of volcanic ash into smectite (Velde, 1995; Murray, 2006). The first two cases (hydrothermal and deuteric alterations) presuppose a primary volcanogenic origin. In fact, smectite-rich volcanoclastic deposits have been recorded in the areas surrounding modern day volcanoes (Fiore, 1993; Mizota and Faure, 1998; Mirabella et al., 2005), confirming the possible formation of smectite directly within active volcanic edifices. In certain cases, the origin of smectite-rich clays is attributed to the alteration of volcanoclastic rocks and lavas emplaced under marine conditions, that is caused by devitrification of the original volcanic glass or by hydrothermal processes (Christidis and Dunham, 1993).

When considering the various proposed interpretations of smectite-rich ashes emitted in the atmosphere by present volcanoes, it is probable that the original volcanoclastic powders contained a significant amount of smectite particles mixed with volcanic glass and quartz, even if a further alteration of the tephra at the sediment/seawater interface, caused by a cation exchange and Mg enrichment (Compton, 1991), cannot be excluded. This may possibly account for admixtures of mixed layers of different nature in the investigated samples.

The mineralogical composition of the bentonites sampled within the Fonzaso Fm. emphasises that the original volcanic ashes were mixed with other intra-basin marine sediments made up of calcite crystals. In fact, the sampled Vajont clays always contained a certain amount of calcite that ranges from low (5–19%) to moderate (23–43%) and high percentages (66%), as shown by the calcimetric analyses (Table 2). The variable mixture of volcanoclastic material with calcareous fine-grained autochthonous sediment originated different mineralogical assemblages, where volcanic ashes predominate (Group 1) or where marine calcite-rich sediments prevail (Group 2), even if an intermediate situation can also occur. These two main mineralogical assemblages can clearly be recognised on examining the geochemical and mineralogical features of the analysed clays (Fig. 9b). Group 1 shows higher percentages of clay minerals (79–96%) associated with considerable amounts of K_2O (2.60–5.77%, in most cases). On the contrary, Group 2 shows lower percentages of interstratified illite/smectite minerals (36–60%), with the lowest values of K_2O (1.17–2.30%).

It is interesting to note that the variable mixture of tephra and marine sediments characterises the single volcanoclastic sedimentation event, so that thin, immediately overlying bentonites can reveal very different relative percentages between volcanic-derived materials and marine calcite-rich sediments. This evidence has been recognised both on the large failure surface of the Vajont landslide (outcrop VA07–3: samples VA07–3A and VA07–3B) and within the lithostratigraphic sequence of Casso (outcrop VA09–1: samples VA09–1A, VA09–1B and VA09–1E), where near-pure volcanoclastic levels are alternated with tephra strongly mixed with marine calcite-rich sediments.

5.3. Provenance

During the Jurassic, there were massive outpourings of basaltic igneous rocks, mass extinctions, significant variations in climate, sea level, atmospheric CO_2 and anoxic episodes (Hesselbo et al., 2002, 2007). Epicontinental seas occupied large parts of western and central Europe by the end of the Early Jurassic. Infilling sediments were predominantly sourced from the east due to the uplift occurring in the East European Platform and the Bohemian massif. According to Ziegler (1990), the rift systems that initiated during the Early Triassic remained active during the Early Jurassic. During the Jurassic period, the southern Tethyan continental margin was affected by extensive tectonics related to *syn*-rift and early post-rift phases while, in the Alpine domain, rifting became increasingly important in the South Alpine and Austroalpine realms even if rift-related volcanism was at a very low level (Ziegler, 1990).

Latin and Waters (1992) and Quirie et al. (2019) reported that moderately to highly alkaline volcanic activity accompanied the formation of the North Sea rift dome in the late Bajocian–Bathonian times. Studies by Berra et al. (2009), Basilone et al. (2010) and others confirmed tectonic control of the Triassic and Jurassic pelagic sediments of the Southern Alps, Apennines and western Sicily. There, submarine to subaerial episodes are reported for the Bajocian–Bathonian (Basilone et al., 2010) while Upper Jurassic is represented by porfiric basalts rich in pyroxenes and plagioclases with rare olivine. Moreover, the Alpine Tethys ophiolitic system (Ligurides / Piedmont / Valais) occurred in late Middle Jurassic time (ca. 185–155 Ma; Lenaz et al., 2019 and references therein).

I/S mixed layer minerals, Ca-smectite, quartz and calcite in different amounts made up the studied materials. Traces of chlorite and kaolinite were present. What could the provenance of these clayey materials be? According to Wang et al. (2013), felsic sources are characterised by low Cr/V and Co/Th ratios and high Y/Ni and La/Sc ratios, while an ophiolitic source would have high amount of Cr and Sc. In the studied

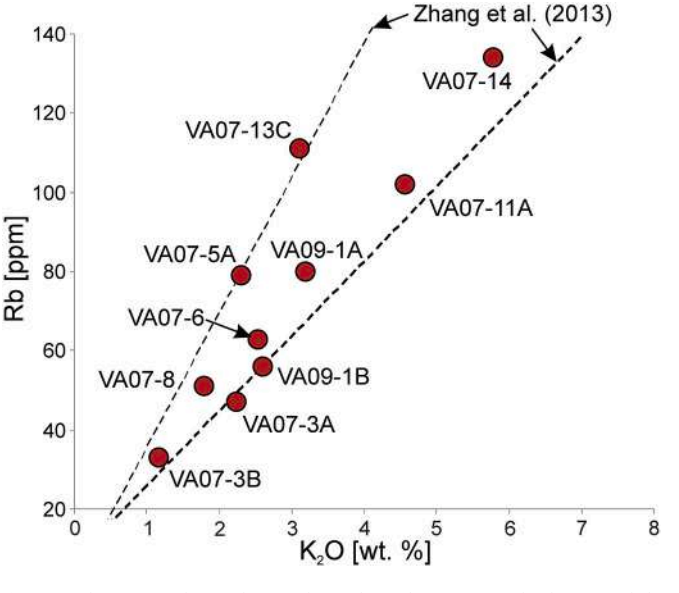

Fig. 10. Rb vs. K_2O chart. The two lines show the mica-trend (above) and the feldspar-trend (below) according to Zhang et al. (2013).

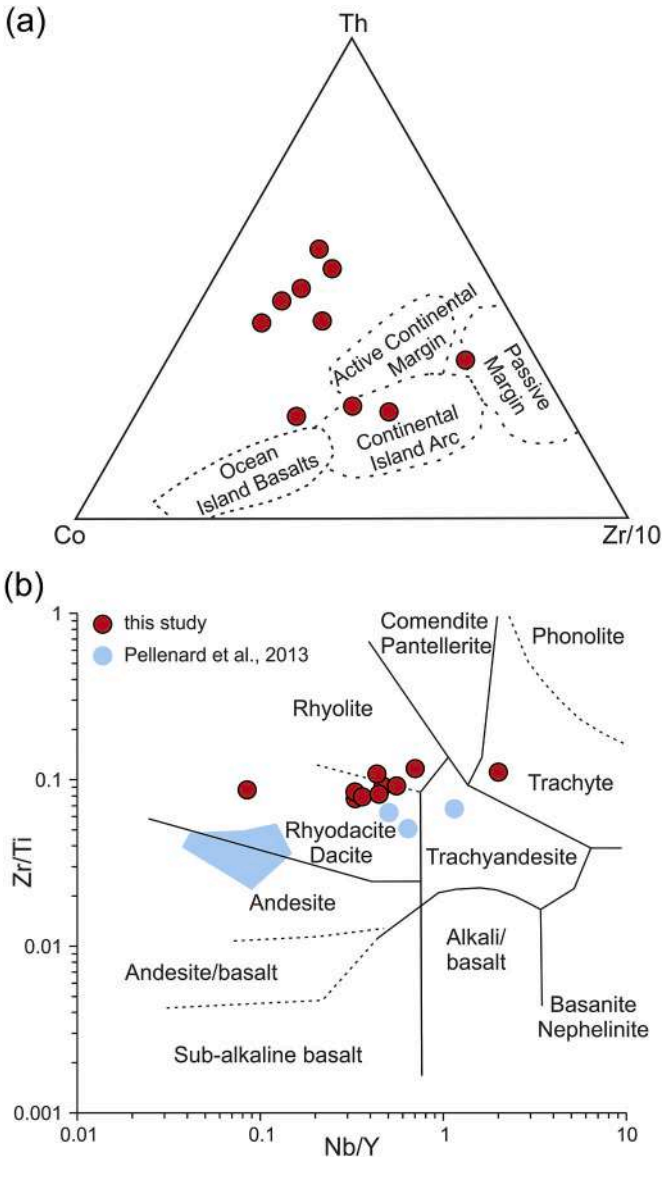

Fig. 11. (a) Th-Co-Zr/10 ternary diagram for the studied samples. Fields after Bhatia and Crook (1986). (b) Zr/Ti vs. Nb/Y diagram for the analysed clay samples from Vajont (red circles). The bentonite layers analysed by Pellenard et al. (2013) are also shown (blue field and circles). Fields after Winchester and Floyd (1977). (For interpretation of the references to colour in this figure legend, the reader is referred to the web version of this article.)

samples, the low Cr content and the Sc content below the detection limit allow us to exclude a mafic source (and consequently the ophiolitic products), pointing to, at least, an intermediate source. This fact is also confirmed by the high amount of Zr. Interestingly, Zhang et al. (2013) suggested that Zn, Ba and Pb could be related to some hydrothermal processes, and Zn and Ba were among the highest trace elements recorded in our samples. Moreover, the same authors recognised the so-called feldspar- and mica-trend relating Rb and K_2O that for our samples suggest a possible derivation from the weathering of micas (Fig. 10).

In order to decipher the possible geological setting for different materials, Bhatia and Crook (1986) proposed the ternary diagram Th-Co-Zr/10. In this diagram, some of our samples fall into the Continental Island Arc field while some others are close to the Active Continental Margin presenting a small Th-excess (Fig. 11a). This could be due to the fact that smectite acts as host for Th (Kelepertsis, 1981; Hein et al., 1982). Low Nb content could be related to a subduction environment (Meijers et al., 2010). Finally, the Zr/Ti vs. Nb/Y diagram (Winchester and Floyd, 1977) suggests a dacite/rhyodacite to rhyolite source, apart from one sample showing a possible trachytic provenance (Fig. 11b).

Geochemical analyses of clayey deposits of Jurassic age are rare. Pellenard et al. (2003) analysed the bentonite deposits of the Oxfordian in the Paris basin and the Callovian–Oxfordian deposits of the Hautes-Alpes department (SE France). Biostratigraphical and geochemical data suggests that the thick bentonite in the Paris Basin correlates with the thickest bentonite in the Subalpine Basin, located 400 km to the south. Those bentonites were characterised by high concentrations of Hf, Nb, Pb, Ta, Th, Ti, U, Y, Zr and low concentrations of Cr, Cs and Rb. Those horizons indicate that significant explosive volcanic events occurred during the Middle Oxfordian. The chemistry of those bentonites corresponds to a trachyandesitic source from a within-plate alkaline series that was probably related to the North Atlantic rifting.

Even if the age is similar, the chemistry of our samples suggests a different source related to a more felsic volcanism. Some smectite-rich clays or bentonites were already recognised in some Upper Jurassic sedimentary sequences of the Italian Alps (Veneto and Trentino regions, northern Italy). In the Ammonitico Rosso Veronese Superiore (ARV_3), Bernoulli and Peters (1970) found thin intercalations of bentonitic clays that they related to a rhyolitic with a tendency to trachytic source. Considering that the material was very fine grained they supposed a distant source (Bernoulli and Peters, 1970).

Eight volcanic ash layers (bentonites) interbedded with marine limestones and cherts were identified in the ARV Formation and were dated to 156.1 ± 0.89 Ma through a ^{40}Ar—^{39}Ar radiometric dating (Pellenard et al., 2013), that is consistent with a late Oxfordian–early Kimmeridgian age. These bentonites were interpreted as volcanoclastic layers linked to large explosive events caused by the subduction-related volcanism from the Vardar Ocean back-arc. The analysed bentonites include “pure smectite horizons” and “occasional volcanic crystals (e.g. sanidine, quartz, biotite)”, but no specific mineralogical analyses of clay minerals were reported (Pellenard et al., 2013). The geochemical signature of the bentonitic levels recognised in the ARV Formation indicates that the primary ash layers derived from an evolved calc-alkaline magma.

Far to the East, the earlier Mesozoic evolution was dominated by

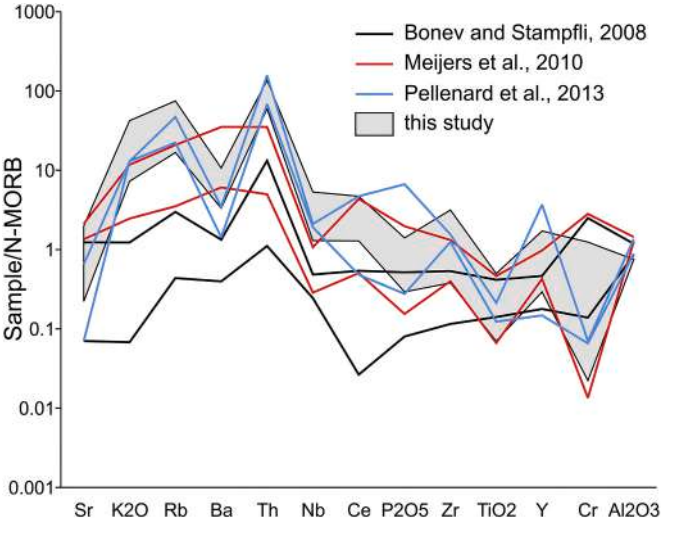

Fig. 12. Comparative spidergrams of trace elements for different materials with a possible common provenance. Fields are displayed considering minimum and maximum contents of the trace elements for each dataset. Black lines: pyroclastic deposits from the Vardar subduction zone (Bonev and Stampfli, 2008); red lines: middle Jurassic dacitic to ryolitic magmas from Crimea (Ukraine) (Meijers et al., 2010); blue lines: late Oxfordian–early Kimmeridgian bentonites from the Ammonitico Rosso Veronese of the Trento Plateau (Pellenard et al., 2013). (For interpretation of the references to colour in this figure legend, the reader is referred to the web version of this article.)

opening and closure of Tethyan oceans between Gondwana and Laurasia with their consumption, at least in part, accommodated along the southern Eurasian margin. Crimea (Ukraine) represents the northernmost region of southeastern Europe that exposes a record of a pre-Cretaceous Tethyan active margin. There, middle Jurassic (~172–158 Ma) and uppermost Jurassic to lowermost Cretaceous (~151–142 Ma) terranes with a subduction-related geochemical signature outcrop (Meijers et al., 2010). Within the Middle Jurassic products, dacitic and ryolitic magmas are present.

For comparison purposes, the spidergrams of trace elements for different materials with a possible common provenance are represented in Fig. 12: (i) the bentonites from Vajont (this study); (ii) the bentonites from the Trento Plateau (Pellenard et al., 2013); (iii) the pyroclastics deposits from the Vardar subduction zone (Bonev and Stampfli, 2008); and (iv) the intermediate to felsic rocks from the Crimea subduction zone (Meijers et al., 2010). As can be seen from the spidergrams, the patterns are rather similar, apart from the trend of the Vardar ones that is almost flat in the part from Nb to Y. Geochemical data of the Vajont bentonites showed a good correspondence with the geochemical fingerprint of the bentonites intercalated in the Ammonitico Rosso Veronese and with the Vardar volcanoclastics, thus a common source and provenance can be hypothesised. However, the Crimea subduction zone could be another possible source of the clay layers occurring in the Vajont sequence.

6. Geotechnical properties vs. mineralogical composition

Grain-size distribution analyses performed on the Vajont clays and reported by Bolla et al. (2020) showed that the investigated clay layers can be described as silty clays and clayey sandy silts, according to the EN ISO 14688 identification and classification of soil. The plasticity properties of these fine soils are rather variable, with the liquid limit (LL) ranging from 38% to 89% and the plasticity index (PI) varying from 21% and 59% (Fig. 13). The plasticity chart of Fig. 13 also correlates the plasticity properties of the Vajont K-bentonites with both their mineralogical composition and the different geological contexts referred to the landslide in which the clay layers occur. When considering the latter issue, the clay lenses localised at the basal contact with the shear zone have an intermediate-to-high plasticity. The tephra levels found in the upper part of the in-situ sequence of the Fonzaso Fm. and the clay layers admixed with the limestone angular gravel have an intermediate plasticity (Fig. 13), even if some samples fall outside the field included between the A-line (Casagrande, 1948) and the U-line (ASTM, 1993).

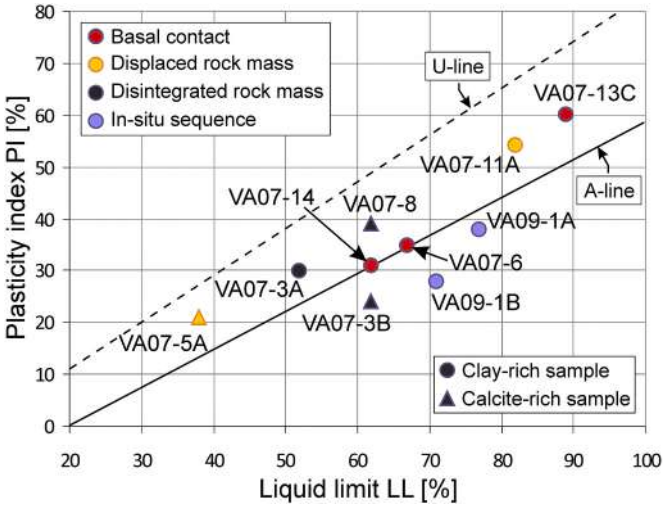

Fig. 13. Plasticity chart of some selected clay samples exhumed from different geological contexts related to the Vajont landslide (modified from Bolla et al., 2020).

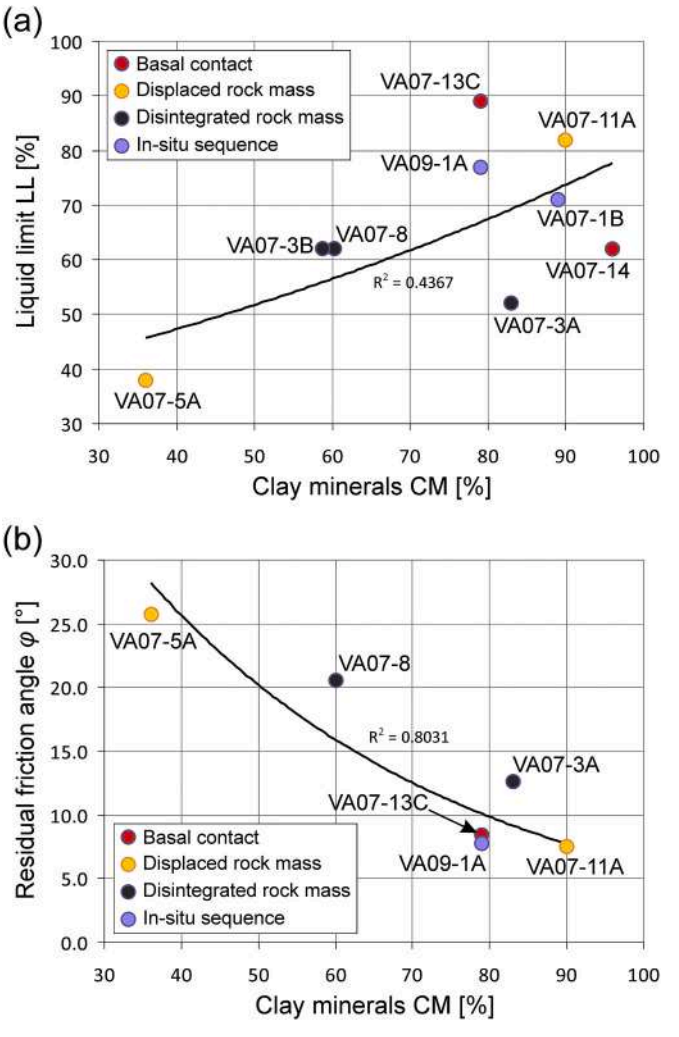

Fig. 14. Correlation diagrams of some Vajont clay samples exhumed from different geological contexts, showing (a) liquid limit vs. clay mineral content and (b) residual friction angle vs. clay mineral content.

Finally, clay interbeds included in the displaced rock masses were found to have highly variable plasticity. However, on the whole, no clear or unambiguous relationship emerges between the plasticity properties and the geological contexts of the sampled soils.

Differently, the plasticity properties of the Vajont clays are clearly influenced by their mineralogical composition. In fact, calcite-rich samples are characterised by an intermediate-to-low plasticity, whereas clay-rich samples have an intermediate-to-high plasticity (Fig. 13). In more detail, the clay mineral content of the fine-grained soils has an influence on their liquid limit, even if a low correlation coefficient characterises the exponential relationship (Fig. 14a). Indeed, clay-rich samples (CM > 79%) are characterised by values of LL ranging from 52% to 89%; whereas samples with a lower content of clay minerals (CM < 60%) have LL values from 38% to 62%. When analysing the different geological contexts related to the landslide, clay layers characterised by intermediate values of the liquid limit (50% < LL < 70%) mainly occur within the disintegrated rock mass of the basal shear zone of the slide. Clay beds with the highest values of LL (71–89%) correspond with the basal sliding surface or in the in-situ limestone sequence at the top of the Fonzaso Fm (Fig. 14a).

Residual shear strength properties of the Vajont K-bentonites were reported by Bolla et al. (2020) in which ring shear tests, performed at 200–600 kPa effective normal stress, revealed a strong influence of the mineralogical composition on the residual shear resistance. In fact, as

visible in the diagram of Fig. 14b, the lowest values of the residual angle of internal friction (7–15°) were obtained for the clay samples with the largest content of clay minerals (CM > 79%), whereas clay layers with a higher content of calcite and quartz were characterised by greater values of the residual friction angle (20–27°). This close relationship is also emphasised by the high correlation coefficient of the exponential trend (Fig. 14b). However, it must also be noted that there is no correlation between the low-shear strength bentonites and the specific geological context in which the clay lenses occur. Indeed, clay-rich soils with low values of the residual angle of internal friction occur indifferently in the in-situ limestone sequence, at the basal failure surface of the slide, within the displaced rock masses and within the disintegrated rock mass of the basal shear zone (Fig. 14b). This evidence has to be kept in mind when analysing the influence exerted by the shear strength properties of the clay interbeds on the specific lithostratigraphic position of the basal failure surface of the Vajont slide.

On the whole, the geotechnical properties of the Vajont clays are strongly dependant on the content of clay minerals within the tephra layers, whereas the specific structure of the I/S mixed layers had no influence on the plasticity and residual shear strength properties of the clays. In fact, the recognised *R*0 and *R*1 Reichweite ordering types and the related illite percentages over smectite (Table 2) characterise both low-plastic and high-plastic clays as well as both low-strength and high-strength clays (Figs. 13 and 14).

7. Geomechanical implications of the tephra layers

The presence of weak illite/smectite mixed layer clays within the Jurassic limestone sequence located at the base of the giant 1963 Vajont landslide has a notable scientific meaning as these bentonitic layers affected the onset and evolution of the large instability processes on the northern slope of Mt. Toc in a decisive manner. During the first studies, the occurrence of these low-strength clay layers was strongly debated due to the limited field evidence for the presence of such materials in the rock sequence, but also because the knowledge about rock masses with intercalated soft clay beds was very poor at that time (1950–1960). The geomechanical implications related to these thin volcanoclastic levels are key for the comprehensive understanding of the evolution of the distinct instability processes that involved the northern slope of Mt. Toc during a time interval of about 18,000–15,000 years, i.e. after the last glacial maximum (LGM).

In fact, the northern slope of Mt. Toc experienced multiple landslide events that can be summarised in (Paronuzzi and Bolla, 2015a): (1) the prehistoric slope failure that occurred in the late Pleistocene–early Holocene and was characterised by a multi-stage rupture including two major primary or first-time failures; and (2) the 9 October 1963 landslide reactivation that remobilised as a single block the previously failed landslide bodies that rested on a basal shear zone of highly variable thickness (10–50 m). Both major landslide events were favoured by three decisive predisposing geological factors: (i) the general dip-slope attitude of bedding planes on the northern slope of Mt. Toc; (ii) the presence of a number of continuous intersecting faults that delimited potentially unstable blocks with a large volume and a near-rectangular shape; and (iii) the occurrence of the high-plastic and low-strength I/S mixed layer clay interbeds within the cherty limestone sequence in the upper half of the Jurassic Fonzaso Fm. The unfavourable combination of these three geological conditions was decisive in causing the first prehistoric slope failures as well as the catastrophic slide that occurred on 9 October 1963. However, due to the very complex geomorphological evolution of the slope, the geomechanical influence of the low-strength bentonitic layers on the slope instability was different, and can only be appreciated on distinguishing the primary failures from the subsequent remobilisation, when the basal shear zone was already created.

The ancient prehistoric Mt. Toc rockslide involved two 100–150 Mm^3-size blocks, i.e., the “Pian del Toc” and “Pian della Pozza” blocks, which collapsed in a consecutive manner originating a partial superimposition of the latter on the back of the former. The time interval that separated these two first-time slope failures is unknown, but their geological similarities seem to indicate a relatively short time interval, and a very rapid retrogressive mechanism can be hypothesised (Paronuzzi and Bolla, 2015a). The recently published (Masè et al., 2004) photographic documentation acquired during the geological survey carried out by Rossi and Semenza immediately after the 1963 landslide, which was favoured by the washing effect caused by the huge waves that impacted the surface of the failed mass, emphasised the presence of the distinct blocks mobilised by the two main prehistoric slope failures. Field evidence proved that these two blocks were affected by strong gravity-induced rock mass damage related to both pre-collapse (quasi-static) and dynamic (run-out) deformation stages (Paronuzzi and Bolla, 2015a).

When relating to the ancient slope failures, the role of the volcanoclastic interbeds was conclusive to the reduction of the available shear strength within the upper sequence of the Fonzaso Fm., thus contributing to the onset of the large slope instability processes. Indeed, due to the very low shear strength of the intercalated bentonitic layers, the initial failure mechanism was strongly controlled by the incipient shear displacements along these weak clay layers. It must now be remarked that, as proved by field evidence, the clay interbeds were 0.5–6.0 cm-thick, in most cases, and had a continuity lower than 10–15 m. When considering the large extent of the bedding planes of the cherty limestone sequence, along with their undulations and sin-sedimentary folding possibly related to Jurassic slumping events, the low thickness and continuity of the clay interbeds caused the occurrence of rock-to-rock contacts along the bedding planes, which represent rigid constraints within the multi-layered sequence.

As a result, relative shear displacements occurring within the bentonitic layers or at the clay–limestone boundary induced localised stress concentrations at the rock-to-rock stiff contacts that caused fracture initiation and propagation at the expense of the limestone beds. The increasing development over time of this characteristic failure mechanism provoked the progressive formation of an incipient shear zone at the base of the unstable slope, with strong rock mass fracturing and/or limestone crushing. Since the volcanoclastic interbeds are concentrated within certain parts of the upper half of the Fonzaso Fm., the critical zone subjected to relative shear slips was not related to a single specific weak clay layer, but rather to a certain stratigraphical sequence including multiple, overlying thin soft clay interbeds. As a consequence, the formation process of the basal shear zone involved a rock mass of considerable depth, reaching the notable thickness of at least 25–30 m.

The multiple I/S mixed layer clays also caused the formation of the typical stepped geometry of the basal failure surface of the Vajont landslide, still visible today on the large failure surface. The multiplicity of weak clay interbeds at the base of the Vajont landslide is not often appreciated, and many geotechnical researchers consider the slope failure as driven by the presence of a single basal low-strength clay layer. On the contrary, the widespread occurrence of thin volcanoclastic clay lenses within the upper sequence of the Fonzaso Fm., which were not limited to a single sedimentary event, was decisive in generating a basal shear zone with a considerable and unexpected thickness. At the same time, from a geomechanical point of view, this peculiarity is a distinctive feature of the Vajont landslide and should be considered when simulating the progressive formation and evolution of the basal shear zone caused by the prehistoric slope failures.

After the occurrence of the prehistoric slope failures, the morphology of the northern slope of Mt. Toc changed substantially, since the two major failed rock blocks stopped at the bottom of the Vajont valley, obstructing the ancient river flow. The 400–500 m-long propagation of the Pian del Toc and Pian della Pozza blocks caused the disruption of the rock mass at the base of the slide, thus developing a mature shear zone made up of abundant limestone angular gravel, sheared-off rock masses and spread clay lenses. As a result, the failed blocks rested on the underlying thick shear zone characterised by newly formed gravelly-type

debris and isolated clay lenses at or near to residual shear strength. This new geological configuration of the slope was completely unknown to the designers of the Vajont dam when the big hydraulic engineering project started and the works officially began on 6 January 1957.

The occurrence of a prehistoric landslide was only suspected in Summer 1960, after the first detailed geological survey of the southern bank of the reservoir (Giudici and Semenza, 1960) and when the precursory signs of slope instability had already been revealed (March 1960). However, the occurrence of an ancient large prehistoric landslide lying on the northern slope of Mt. Toc was strongly confuted by other experts, both geotechnical engineers and geologists, that were consulted at that time to interpret and to manage the forthcoming large slope instability, which was dramatically heralded by the huge threatening fissure, the well known "M-shaped" crack, which suddenly occurred in late October–early November 1960.

The catastrophic collapse of 9 October 1963 was a classic example of remobilisation of an ancient landslide, which was induced by three repeated filling–drawdown cycles of the reservoir that were performed, with some interruptions, from 2 February 1960, and was followed by the unforeseen en-block sliding motion. During this man-induced landslide remobilisation, the geomechanical role of volcanoclastic interbeds was different, when compared with the influence of the clays in activating the first-time slope failures related to the prehistoric instability. As a result of the rock mass comminution at the base of the slide, the clay layers formed very irregular and discontinuous lenses with moderate planar extension, and the shear zone material was dominated by the highly permeable limestone angular gravel. This means that the clay layers represented isolated thin lenses without any effect on the overall hydraulic conductivity of the shear zone material. The pore water pressure changes induced by the reservoir level fluctuations were exclusively influenced by the high permeability of the gravelly soils, without any actual sealing effect provided by the isolated clay lenses.

At the time of the final slope instability, most clay lenses were at or near residual shear strength due to the considerable displacements that had previously accumulated as a consequence of the prehistoric failures. Obviously, the low-resistance I/S clay lenses contributed to reducing the available shear strength along the future failure surface of the 1963 slide, which partially formed within the shear zone material and partially reworked the dip-slope bedding planes of the Fonzaso Fm. (Fig. 3). However, the decisive landslide trigger was the rise in the pore water pressures along the failure surface, in particular the decrease in the effective stresses caused by the groundwater inflow related to the reservoir impoundments. This means that the role of the volcanoclastic clays was secondary or subordinate in the occurrence of the catastrophic 1963 landslide remobilisation, whereas in this circumstance, the presence of the highly permeable limestone angular gravel of the shear zone was decisive.

8. Conclusions

The presence of soft clay layers intercalated within the Fonzaso Fm. dated to the Upper Jurassic was an unexpected geological feature and, for this reason, was strongly debated by the first researchers dealing with the Vajont landslide, especially by Leopold Müller, the major geotechnical engineer involved in the construction of the hydroelectric power plant at Vajont. This is not surprising, especially if we consider the state of the geological and geotechnical knowledge dating back in 1960 or immediately after. The presence of a prehistoric rockslide lying on the northern slope of Mt. Toc was and, for some researchers, still is a contended issue. Although the 1963 Vajont landslide has been analysed from different scientific points of view, previous studies never examined the problem of the particular mineralogical nature of the clays involved in the slope rupture and, in particular, their geological origin and provenance.

The mineralogical investigations of the clay interbeds occurring within the Fonzaso Fm. and outcropping in the Vajont valley showed the occurrence of complex assemblages of illite/smectite (I/S) mixed layers admixed with variable amounts of calcite and quartz (Bolla et al., 2020). On the whole, the investigated clay samples were characterised by highly variable contents of clay minerals (CM = 36–96%), calcite (Cal = 4–64%) and quartz (Qtz = 0–6%). However, *R*0 and *R*1 Reichweite ordering types were recognised, with an illite content ranging from 50% up to 85%, suggesting a low-to-medium degree of smectite-to-illite diagenetic transformation. The abundance of illite in the mixed-layers assemblage is confirmed by the high percentage of potassium as revealed by the geochemical analyses of the sampled clays.

On the basis of the study carried out, the clays interbeds included in the Jurassic Fonzaso Fm. outcropping in the Vajont valley are the final result of a temporal sequence of complex geological phenomena, including:

(1) initial eruption and injection into the atmosphere of volcanic ash;
(2) transport by wind and subsequent sedimentation in the Jurassic Vajont Basin; and.
(3) weathering and/or alteration of the original volcanoclastic material caused by diagenesis and burial-related phenomena.

Fine-textured volcanogenic materials were transported by wind over a long distance from the explosive source (in the order of 1000–3000 km), probably from the Vardar Ocean back-arc or from the Crimea (Ukraine) subduction zone, and then were deposited in the Jurassic Vajont Basin.

Field evidence shows that:

(1) the oldest strata in the first 10–15 m of the cherty limestone sequence of the Fonzaso Fm. (dating to middle Callovian–middle Oxfordian) do not include any clay layers;
(2) multiple thin tephra layers concentrate in some specific 1–2 m-thick rock strata sequences occurring in the upper succession of FOZ (late Oxfordian–upper Tithonian) and were involved in the large basal rupture;
(3) clay layers are discontinuous (maximum ascertained continuity: 10–15 m) and can be identified, near exclusively, in some specific geological contexts: (i) the basal failure surface and (ii) the displaced and disintegrated rock mass related to the shear zone formation.

The occurrence of several distinct, very thin, clay-rich layers influenced the position of the basal failure surface of the Vajont landslide and caused its typical stepped morphology. The stratigraphic influence on the position of the basal rupture surface is strictly correlated with the occurrence of the first tephra layers within the Fonzaso Fm. In fact, the mineralogical and geochemical analyses showed that the clay layers sampled at the basal contact between the sliding surface and the shear zone were characterised by a higher content of clay minerals (Fig. 9) and had a considerable amount of illite/smectite mixed layers. Interestingly, clay layers occurring on the eastern part of the detachment surface are characterised by high percentages of clay minerals (Fig. 9) and show a higher diagenetic maturity (Table 2) when compared with clays sampled from the western failure scar. This suggests that the clay layers in the eastern (older strata) and western (younger strata) parts of the large basal failure surface belong to different parts of the geological sequence (Fig. 3).

The mineralogical composition of the clay layers had a strong influence on their geotechnical properties, and in particular, on the value of the residual angle of internal friction (φ_{res}). In fact, clay interbeds with a large prevalence of clay minerals (CM > 79%) are characterised by low values of φ_{res} (6.7–14.9°); whereas clayey materials with a large content of granular minerals (calcite and quartz) have greater values of φ_{res} (19.5–26.7°). The mechanical role played by these soft clay interbeds in the instability processes that involved the northern slope of Mt. Toc over time was different when considering the prehistoric rockslide and the 1963 en-block remobilisation.

When considering the ancient slope failures and the primary structure of the multi-layered rock mass, the occurrence of concentrated clay interbeds within some specific rock strata sequences resulted in a localised decrease in the available shear strength, enabling relative shear displacements along the dip-slope bedding planes. To accommodate the deformation induced by the incipient instability condition of the slope, cross-cutting fractures caused by tensile and secondary shear stresses formed within the 5–10 cm-thick limestone beds, thus determining the enucleation and propagation of multiple internal shear/tensile rupture surfaces. As a result, the basal failure surface of the prehistoric rockslides, which was subsequently re-worked during the 1963 remobilisation, had a complex stepped shape, involving several distinct clay-rich layers.

Differently, when considering the instability process that involved the Mt. Toc slope during the operating period of the hydroelectric power plant (1960–1963) and that culminated with the catastrophic failure on 9 October 1963, the mechanical influence of the clay layers is strictly related to a decrease in the average shear strength due to previous displacements on the basal shear zone of the slide. In fact, the basal failure mechanism of the 1963 Vajont slide was complex and involved various geological materials: spread bentonitic layers of variable residual shear strength, rock joints, cherty limestone beds and a prevailing amount of limestone angular gravel. This means that the shear strength of the basal rupture zone cannot be only related to the residual shear resistance of the weakest materials, i.e. of the bentonites with a higher content of clay minerals; but the shear strength of the other materials involved in the basal rupture has to be considered. This also explains how a single "critical" low-resistance clay layer at the base of the slide (Hendron and Patton, 1985) represents an inadequate geotechnical simplification.

The 1963 Vajont landslide provides an excellent case-history to learn that it is always necessary to balance detailed basic geological knowledge (geomorphology, lithostratigraphy and structural geology) with further slope stability analyses and/or advanced numerical modelling. This is true even though almost 60 years have passed since the catastrophic event, and that hard lesson remains valid, both for engineers and geologists. Currently, progress in scientific research has widely proved the possible occurrence of volcanoclastic clays within sedimentary sequences of the Mesozoic or even Paleozoic age, and this has been well exemplified by some tephra levels identified thanks to a lithostratigraphic field survey performed in various geological contexts around the world (Huff, 2016). For this reason, the soft I/S mixed layer clays characterising the base of the Vajont landslide do not represent an impossible geological situation, as thought many years ago by Müller, but rather a complex stratigraphical circumstance that can only be recognised after a very accurate field survey. Analogously, the occurrence of huge prehistoric landslides on alpine valleys, most of which occurred after LGM or during the early Holocene, is a geological evidence that is widely accepted today by the scientific community (Heim, 1932; Abele, 1974; Prager et al., 2008; McColl, 2012), and the prehistoric Vajont landslide is only one example of the many case-histories recorded in various geographical contexts where ancient slope failures were driven by concomitant predisposing geological factors.

Clay-rich interbeds within sedimentary sequences, especially those including smectite and/or mixed layers clays with low shear strength, represent a typical example in which a relatively minor geological feature has a major impact on the behaviour of the rock mass and the related slope stability condition (e.g., Tommasi et al., 2009; Esposito et al., 2013; Massey et al., 2013; Tonelli et al., 2019). As this paper demonstrates, the genesis and geological formation processes of clay interbeds have a strong influence on their geometrical shape, lithostratigraphic position in the rock sequence, mineralogical characteristics and, in turn, geotechnical properties, which exert significant controls over the slope failure mechanism and type of movement.

As a concluding remark, it can be emphasised that the traditional geological field survey maintains its basic importance to investigate previous landslides or slope instability processes adequately, and this is particularly true for very complex geological situations, as the catastrophic Vajont landslide demonstrates. Sophisticated numerical modelling can never compensate for the poor quality of the geological investigation, and the weakness of basic knowledge or even preconceived ideas can strongly affect the correct interpretation of a rock slope stability problem.

Funding

This research received no specific grant from any funding agency in the public, commercial, or not-for-profit sectors.

Authors' contribution

Authors make substantial contributions to conception and design, and/or acquisition of data, and/or analysis and interpretation of data.

Author statement

Alberto Bolla on behalf of the authors states that all authors have seen and approved the final version of the manuscript being submitted. We warrant that the article is the authors' original work, hasn't received prior publication and isn't under consideration for publication elsewhere.

Declaration of Competing Interest

The authors declare that they have no competing interests or personal relationships that could have appeared to influence the work reported in this paper.

References

Abele, G., 1974. Bergstürze in den Alpen: ihre Verbreitung, Morphologie und Folgeerscheinungen. Wissenschlaftliche Alpenvereinshefte, 25. München, p. 230.

Alonso, E.E., Pinyol, N.M., 2010. Criteria for rapid sliding: I. a review of Vaiont case. Eng. Geol. 114, 198–210.

American Society for Testing and Materials, 1993. Standard classification of soils for engineering purposes. Test Designation D2487, Volume 04.08. Available online at: https://www.astm.org/Standards/D2487 (accessed on 10 July 2021).

Árkai, P., 2002. Phyllosilicates in very low-grade metamorphism: Transformation to micas. In: Mottana, A., Sassi, F.P., Thomson, J.B., Guggenheim, S. (Eds.), Micas: Crystal Chemistry and Metamorphic Petrology. Mineralogical Society of America, Reviews in Mineralogy and Geochemistry 46, pp. 463–478.

Basilone, L., Morticelli, M.G., Lena, G., 2010. Mesozoic tectonics and volcanism of Tethyan rifted continental margins in western Sicily. Sediment. Geol. 226, 54–70.

Bernoulli, D., Peters, T., 1970. Traces of rhyolitic-trachytic volcanism in the Upper Jurassic of the Southern Alps. Eclogae Geol. Helv. 63, 609–621.

Berra, F., Galli, M.T., Reghellin, F., Torricelli, S., Fantoni, R., 2009. Stratigraphic evolution of the Triassic-Jurassic succession in the Western Southern Alps (Italy): the record of the two-stage rifting on the distal passive margin of Adria. Basin Res. 21, 335–353.

Bethke, C.M., Vergo, N., Altaner, S., 1986. Pathways of smectite illitization. Clay Clay Miner. 34 (2), 125–135.

Bhatia, M.R., Crook, K.A.W., 1986. Trace element characteristics of graywackes and tectonic setting discrimination of sedimentary basins. Contrib. Mineral. Petrol. 92, 181–193.

Bolla, A., Paronuzzi, P., Pinto, D., Lenaz, D., Del Fabbro, M., 2020. Mineralogical and geotechnical characterization of the clay layers within the basal shear zone of the 1963 Vajont landslide. Geosciences 10 (9), 360.

Bonev, N., Stampfli, G., 2008. Petrology, geochemistry and geodynamic implications of Jurassic island arc magmatism as revealed by mafic volcanic rocks in the Mesozoic low-grade sequence, eastern Rhodope, Bulgaria. Lithos 100, 210–233.

Broili, L., 1967. New knowledges on the geomorphology of the Vaiont slide slip surfaces. Rock Mech. Eng. Geol. 5, 38–88.

Casagrande, A., 1948. Classification and identification of soils. Trans. ASCE 113, 901–991.

Christidis, G., Dunham, A.C., 1993. Compositional variations in smectites: part I. Alteration of intermediate volcanic rocks. A case study from Milos Island, Greece. Clay Miner. 28, 255–273.

Compton, J.S., 1991. Origin and diagenesis of clay minerals in the Monterey Formation, Santa Maria basin area, California. Clay Clay Miner. 39, 449–466.

Cuadros, J., Altaner, S., 1998. Characterization of mixed-layer illite-smectite from bentonites using microscopic, chemical and X-ray methods: constraints on the smectite-to-illite transformation mechanism. Am. Mineral. 83, 762–774.

Dykes, A.P., Bromhead, E.N., 2018. The Vaiont landslide: re-assessment of the evidence leads to rejection of the consensus. Landslides 15, 1815–1832.

Eslinger, E., Pevear, D.R., 1988. Clay Minerals for Petroleum Geologists and Engineers. SEPM Short Course No. 22. Society for Sedimentary Geology, Tulsa, USA, p. 428.
Esposito, C., Bianchi-Fasani, G., Martino, S., Scarascia-Mugnozza, G., 2013. Quaternary gravitational morpho-genesis of Central Apennines (Italy): insights from the Mt. Genzana case history. Tectonophysics 605, 96–103.
Fang, Q., Churchman, G.J., Hong, H., Chen, Z., Liu, J., Yu, J., Han, W., Wang, C., Zhao, L., Furnes, H., 2017. New insights into microbial smectite illitization in the Permo-Triassic boundary K-bentonites, South China. Appl. Clay Sci. 140, 96–111.
Ferri, F., Di Toro, G., Hirose, T., Han, R., Noda, H., Shimamoto, T., Quaresimin, M., de Rossi, N., 2011. Low- to high-velocity frictional properties of the clay-rich gouges from the slipping zone of the 1963 Vaiont slide, northern Italy. J. Geophys. Res. 116, B09208 https://doi.org/10.1029/2011JB008338.
Fiore, S., 1993. The occurrences of smectite and illite in a pyroclastic deposits prior to weathering: implications on the genesis of 2:1 clay minerals in volcanic soils. Appl. Clay Sci. 8, 249–259.
Giudici, F., Semenza, E., 1960. Studio geologico sul serbatoio del Vajont. Unpublished report for SADE, Venezia, Italy, 63 pp.
Heim, A., 1932. Bergsturz und Menschenleben. Zürich Fretz & Wasmuth Verlag, Zürich, p. 218 (In German).
Hein, J.R., Koski, R.A., Morgenson, L.A., 1982. Uranium and thorium enrichment in rocks from the base of DSDP Hole 465A, Hess rise, central North Pacific. Chem. Geol. 36, 237–251.
Hendron, A.J., Patton, F.D., 1985. The Vaiont slide, a geotechnical analysis based on new geologic observations of the failure surface. In: Technical Report GL-85-5. Department of the Army, U.S. Army Corps of Engineers, Washington, DC.
Hesselbo, S.P., Robinson, S.A., Surlyk, F., Piasecki, S., 2002. Terrestrial and marine extinction at the Triassic-Jurassic boundary synchronized with major carbon-cycle perturbation: a link to initiation of massive volcanism? Geology 30, 251–254.
Hesselbo, S.P., Jenkyns, H.C., Duarte, L.V., Oliveira, L.C.V., 2007. Carbon-isotope record of the early Jurassic (Toarcian) Oceanic Anoxic Event from fossil wood and marine carbonate (Lusitanian Basin, Portugal). Earth Planet. Sci. Lett. 253, 455–470.
Huang, W.-L., Longo, J.M., Pevear, D.R., 1993. An experimentally derived kinetic model for smectite-to-illite conversion and its use as a geothermometer. Clay Clay Miner. 41, 162–177.
Huff, W.D., 2016. K-bentonites: a review. Am. Mineral. 101, 43–70.
Inoue, A., Lanson, B., Marques-Fernandes, M., Sakharov, B.A., Murakami, T., Meunier, A., Beaufort, D., 2005. Illite-smectite mixed-layer minerals in the hydrothermal alteration of volcanic rocks: I. One-dimensional XRD structure analysis and characterization of component layers. Clay Clay Miner. 53 (5), 423–439.
Kelepertsis, A.E., 1981. The geochemistry of uranium and thorium in some lower Carboniferous sedimentary rocks (Great Britain). Chem. Geol. 34, 275–288.
Kenney, T.C., 1967. The influence of mineral composition on the residual strength of natural soils. In: Proceedings of Geotechnical Conference. Oslo(1), pp. 123–129.
Kenney, T.C., 1992. Slope stability in artificial reservoirs: Influence of reservoir level, selected cases, and possible solutions. In: Semenza, E., Melidoro, G. (Eds.), Proceedings of the Meeting on the 1963 Vaiont Landslide, 17–19 September 1986, Ferrara. Cansiglio and Vaiont. Grafica Ferrarese, Ferrara, Italy, pp. 67–85.
Kiersch, G.A., 1964. Vaiont reservoir disaster. Civ. Eng. 34, 32–39.
Lanson, B., Sakharov, B.A., Claret, F., Drits, V.A., 2009. Diagenetic illite-to-smectite transition in clay-rich sediments: a reappraisal of x-ray diffraction results using the multi-specimen method. Am. J. Sci. 309, 476–516.
Latin, D., Waters, F., 1992. Basaltic magmatism in the North Sea and its relationship to lithospheric extension. Tectonophysics 208, 77–90.
Lenaz, D., Schmitz, B., Alvarez, W., 2019. Terrestrial Cr-spinels in the Maiolica limestone: Where are they from? In: Koeberl, C., Bice, D.M. (Eds.), 250 Million Years of Earth History in Central Italy: Celebrating 25 Years of the Geological Observatory of Coldigioco. Geological Society of America Special Paper 542, pp. 121–131.
Lo, K.Y., Lee, C.F., Gélinas, P., 1972. Alternative interpretation of the Vaiont slide. In: Cording, E.J. (Ed.), Stability of Rock Slopes. Proc. 13th Symp. On Rock Mechanics, Univ. Illinois, Urbana. ASCE, New York, pp. 595–623.
Mantovani, F., Vita-Finzi, C., 2003. Neotectonics of the Vajont dam site. Geomorphology 54, 33–37.
Martinis, B., 1978. Contributo alla stratigrafia dei dintorni di Erto-Casso (Pordenone) ed alla conoscenza delle caratteristiche strutturali e meccaniche della frana del Vajont. Mem. Sci. Geol. Univ. Padova 32, 1–33.
Masè, G., Semenza, M., Semenza, P., Semenza, P., Turrini, M.C., 2004. Le foto della frana del Vajont. Edizioni k-flash, Ferrara, Italy (3 maps and CD-ROM, 650 MB).
Massey, C.I., Petley, D.N., McSavaney, M.J., 2013. Patterns of movement in reactivated landslides. Eng. Geol. 159, 1–19.
McColl, S.T., 2012. Paraglacial rock-slope stability. Geomorphology 153-154, 1–16.
Meijers, M.J.M., Vrouwe, B., van Hinsbergen, D.J.J., Kuiper, K.F., Wijbrans, J., Davies, G. R., Stephenson, R.A., Kaymak, N., Matenco, L., Saintot, A., 2010. Jurassic arc volcanism on Crimea (Ukraine): implications for the paleo-subduction zone configuration of the Black Sea region. Lithos 119, 412–426.
Merriman, R.J., 2005. Clay minerals and sedimentary basin history. Eur. J. Mineral. 17, 7–20.
Merriman, R.J., Peacor, D.R., 1999. Very low-grade metapelites: Mineralogy, microfabrics and measuring reaction progress. In: Frey, M., Robinson, D. (Eds.), Low-Grade Metamorphism. Blackwell Science, Oxford, pp. 10–60.
Mirabella, A., Egli, M., Raimondi, S., Giaccai, D., 2005. Origin of clay minerals in soils on pyroclastic deposits in the island of Lipari (Italy). Clay Clay Miner. 53 (4), 409–421.
Mizota, C., Faure, K., 1998. Hydrothermal origin of smectite in volcanic ash. Clay Clay Miner. 46 (2), 178–182.
Moore, D.M., Reynolds Jr., R.C., 1997. X-Ray Diffraction and the Identification and Analysis of Clay Minerals, 2nd edition. Oxford University Press, New York. 332 pp.
Müller, L., 1964. The rock slide in the Vajont valley. Rock Mech. Eng. Geol. 2, 148–212.
Müller, L., 1968. New considerations on the Vaiont slide. Rock Mech. Eng. Geol. 6, 1–91.
Murray, H.H., 2006. Applied Clay Mineralogy. In: Occurrences, Processing and Applications of Kaolins, Bentonites, Palygorskitesepiolite, and Common Clays. Elsevier Science, 188 pp.
Nonveiller, E., 1967. Shear strength of bedded and jointed rock as determined from the Zalesina and Vajont slides. In: Proceedings of Geotechnical Conference, Oslo, Norway. Norwegian Geotechnical Institute, 1, pp. 289–294.
Paronuzzi, P., Bolla, A., 2012. The prehistoric Vajont rockslide: an updated geological model. Geomorphology 169-170, 165–191.
Paronuzzi, P., Bolla, A., 2013. A new interpretation of the geotechnical context of the Vajont rockslide. In: Margottini, C., Canuti, P., Sassa, K. (Eds.), Landslide Science and Practice: Risk Assessment, Management and Mitigation. Proceedings of the Second World Landslide Forum, 3-9 October 2011, Rome, Italy. Springer, Berlin, Germany, pp. 123–132.
Paronuzzi, P., Bolla, A., 2015a. Gravity-induced rock mass damage related to large en masse rockslides: evidence from Vajont. Geomorphology 234, 28–53.
Paronuzzi, P., Bolla, A., 2015b. Gravity-induced fracturing in large rockslides: possible evidence from Vajont. In: Lollino, G., Giordan, D., Crosta, G.B., Corominas, J., Azzam, R., Wasowski, J., Sciarra, N. (Eds.), Engineering Geology for Society and Territory: Landslide Processes. Proceedings of the XII International IAEG Congress, 15–19 September 2014, Turin, Italy. Springer, pp. 213–216.
Paronuzzi, P., Rigo, E., Bolla, A., 2013a. Influence of filling–drawdown cycles of the Vajont reservoir on Mt. Toc slope stability. Geomorphology 191, 75–93.
Paronuzzi, P., Rigo, E., Bolla, A., 2013b. A coupled seepage-stability model to analyze the Vajont reservoir influence. In: Margottini, C., Canuti, P., Sassa, K. (Eds.), Landslide Science and Practice: Risk Assessment, Management and Mitigation. Proceedings of the Second World Landslide Forum, 3-9 October 2011, Rome, Italy. Springer, Berlin, Germany, pp. 97–106.
Paronuzzi, P., Bolla, A., Rigo, E., 2016. Brittle and ductile behavior in deep-seated landslides: learning from the Vajont experience. Rock Mech. Rock. Eng. 49 (6), 2389–2411.
Pellenard, P., Deconinck, J.-F., Huff, W.D., Thierry, J., Marchand, D., Fortwengler, D., Trouiller, A., 2003. Characterization and correlation of Upper Jurassic (Oxfordian) bentonite deposits in the Paris Basin and the Subalpine Basin, France. Sedimentology 50, 1035–1060.
Pellenard, P., Nomade, S., Martire, L., De Oliveira Ramalho, F., Monna, F., Guillou, H., 2013. The first 40Ar–39Ar date from Oxfordian ammonite-calibrated volcanic layers (bentonite) as a tie-point for the late Jurassic. Geol. Mag. 150 (6), 1136–1142.
Prager, C., Zangerl, C., Patzelt, G., Brandner, R., 2008. Age distribution of fossil landslides in the Tyrol (Austria) and its surrounding areas. Nat. Hazards Earth Syst. Sci. 8, 377–407.
Pytte, A.M., Reynolds, R.C., 1989. The thermal transformation of smectite to illite. In: Naeser, N.D., McCulloh, T.H. (Eds.), Thermal History of Sedimentary Basins. Springer-Verlag, Berlin, pp. 133–140.
Quirie, A.K., Schofield, N., Hartley, A., Hole, M.J., Archer, S.G., Underhill, J.R., Watson, D., Holford, S.P., 2019. The Rattray Volcanics: Mid-Jurassic fissure volcanism in the UK Central North Sea. J. Geol. Soc. 176, 462–481.
Selli, R., Trevisan, L., 1964. Caratteri e interpretazione della Frana del Vaiont. Giorn. Geol. 32, 7–104.
Skempton, A.W., 1966. Bedding-plane slip, residual strength and the Vaiont landslide. Géotechnique 16 (1), 82–84.
Spinola, D.S., Pi-Puig, T., Solleiro-Rebolledo, E., Egli, M., Sudo, M., Sedov, S., Kűhn, P., 2017. Origin of clay minerals in early Eocene volcanic palaeosols on King Gorge Island, Maritime Antarctica. Nat. Sci. Rep. 7, 6368. https://doi.org/10.1038/s41598-017-06617-x.
Tika, T.H.E., Hutchinson, J.N., 1999. Ring shear tests on soil from the Vaiont slide slip surface. Géotechnique 49 (1), 59–74.
Tommasi, P., Verrucci, L., Campedel, P., Veronese, L., Pettinelli, E., Ribacchi, R., 2009. Buckling of high natural scope: the case of Lavini di Marco (Trento-Italy). Eng. Geol. 109, 93–108.
Tonelli, G., Veneri, F., Mattioli, M., Paletta, C., 2019. The role of a bentonitic layer on slope stability in bedded limestone: the case study of the December 2004 Ca' Madonna Quarry rock slide (Umbria-Marche Apennines, Central Italy). Ital. J. Geosci. 138, 56–65.
Velde, B., 1995. Origin and Mineralogy of Clays. Clays and the Environment. Springer-Verlag, p. 334.
Wang, B.-Q., Wang, W., Zhou, M.F., 2013. Provenance and tectonic setting of the Triassic Yidun Group, the Yidun Terrane. Tibet. Geosci. Front. 4, 765–777.
Weibel, R., 1999. Effects of burial on the clay assemblages in the Triassic Skagerrak Formation, Denmark. Clay Miner. 34, 619–635.
Winchester, J.A., Floyd, P.A., 1977. Geochemical discrimination of different magma series and their differentiation products using immobile elements. Chem. Geol. 20, 325–343.
Wolter, A., Stead, D., Clague, J.J., 2014. A morphological characterisation of the 1963 Vajont Slide, Italy, using long-range terrestrial photogrammetry. Geomorphology 206, 147–164.
Wolter, A., Stead, D., Ward, B.C., Clague, J.J., Ghirotti, M., 2016. Engineering geomorphological characterisation of the Vajont Slide, Italy, and a new interpretation of the chronology and evolution of the landslide. Landslides 13, 1067–1081.
Zhang, Y., Pe-Piper, G., Piper, D.J.W., 2013. Sediment geochemistry as a provenance indicator: Unravelling the cryptic signatures of polycyclic sources, climate change, tectonism and volcanism. Sedimentology 61, 383–410.
Ziegler, P.A., 1990. Geological Atlas of Western and Central Europe, 2nd edition. Shell International Petroleum Mij. B.V. and Geological Society, London. 239 pp.